ORGANOMETALLICS

Article

pubs.acs.org/Organometallics

# Synthesis of *N*-Aryloxy-β-diketiminate Ligands and Coordination to Zirconium, Ytterbium, Thorium, and Uranium

Florian Dulong, Pierre Thuéry, Michel Ephritikhine, and Thibault Cantat*

CEA, IRAMIS, SIS2M, CNRS UMR 3299, CEA/Saclay, 91191 Gif-sur-Yvette, France

Supporting Information

**ABSTRACT:** Two examples of *N*-aryloxy-β-diketiminate dianions (**11a,b**) have been synthesized on a multigram scale, in four steps, from commercially available chemicals. The synthetic scheme relies on the sequential addition of 2,6-diisopropylaniline and 2-amino-4-*tert*-butylphenol (**1a**) (or 2-amino-4,6-di-*tert*-butylphenol (**1b**)) to acetylacetone, using $Et_3OBF_4$ as an activation reagent. Both the nature of the activation reagent and the order of addition of the primary amines have a major impact on the outcome of the reaction, and acid catalysts (such as sulfuric acid or *p*-toluenesulfonic acid) lead to decomposition of the β-diketiminate backbone via formation of a benzoxazole derivative (**3a,b**). Using dianions **11a,b**, mono- and bis(*N*-aryloxy-β-diketiminate) complexes of zirconium(IV), ytterbium(III), thorium(IV), and uranium(IV) have been synthesized (**12**−**18**), by salt metathesis reactions, and characterized by a combination of $^1H/^{13}C$ NMR spectroscopy, elemental analysis, and X-ray crystallography. The two ligands differ in their steric bulk and exhibit different coordination behaviors, which were rationalized on the basis of geometric considerations.

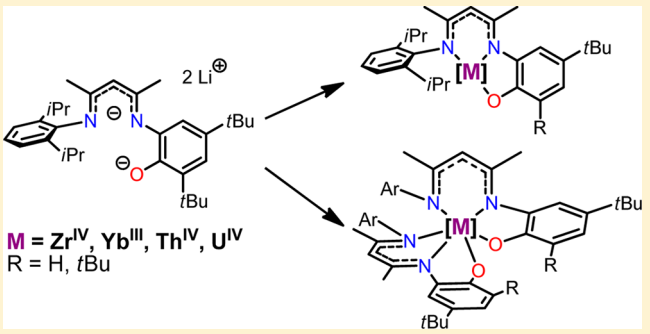


## INTRODUCTION

β-Diketiminate ligands, the nitrogen analogues of β-diketonate ligands, have received increased interest and found important applications in coordination chemistry and homogeneous catalysis because changing the substituents on the nitrogen atoms enables a fine tuning of the ligand electronic and geometric properties.[1−4] For example, sterically encumbered β-diketiminates are efficient ancillary ligands to support coordinatively and electronically unsaturated complexes that were successfully utilized as catalysts in the polymerization of ethylene and propene.[5,6] Capitalizing on the properties of this ligands class, novel pincer ligands have been synthesized, by introducing neutral donors (e.g., ethers and amines) on the nitrogen substituents of the β-diketiminate backbone.[7,8] Yet, examples of di- or trianionic polydentate β-diketiminate structures featuring an anionic alkoxide or amide functionality remain scarce.[9−11] In order to circumvent this limitation, we have recently reported the first example of a *N*-aryloxy-β-diketiminate ligand and explored its coordination chemistry with electron-poor metal ions.[11] Herein, we propose a rational synthesis of this new class of ligands which is exemplified by the preparation of two types of *N*-aryloxy-β-diketiminate ligands with different steric bulk. Their different coordination behaviors with zirconium(IV), ytterbium(III), thorium(IV), and uranium(IV) metal ions is presented.

## RESULTS AND DISCUSSION

**Synthesis of *N*-Aryloxy-β-diketiminate Ligands.** β-Diketiminate ligands are routinely prepared by double condensation of primary amines onto 2,4-pentanedione using simple acids as catalysts, such as hydrochloric acid, sulfuric acid, and *p*-toluenesulfonic acid (PTSA).[1,7,12] However, in a preliminary contribution, we observed that introduction of nucleophilic functional groups (e.g., a phenol group) on the amine backbone proved problematic and prevented the formation of the desired β-diketiminate structure.[11] In order to shed light on the origins of this chemical behavior and expand the scope of available *N*-aryloxy-β-diketiminate ligands (see targeted structures in Scheme 1), we have investigated in detail the reaction chemistry between *o*-aminophenol derivatives **1** and acetylacetone, under cationic activation. 2-Amino-4-*tert*-butylphenol (R = H, **1a**) and 2-amino-4,6-di-*tert*-butylphenol (R = *t*Bu, **1b**) were considered as functionalized aniline derivatives in order to access *N*-aryloxy-β-diketiminate ligands with different steric bulks and, therefore, tune the steric

**Scheme 1. Targeted *N*-Aryloxy-β-diketiminate Ligands**

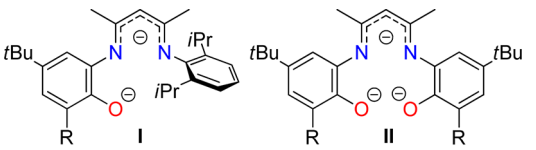


Special Issue: Recent Advances in Organo-f-Element Chemistry

Received: October 31, 2012
Published: January 23, 2013

   dx.doi.org/10.1021/om3010355 | *Organometallics* 2013, 32, 1328−1340

congestion at the metal center upon coordination. Condensation of **1** with acetylacetone is thermally available and affords the acnac pro-ligands **2** in high yields without catalytic assistance (Scheme 2, eq 1). **2** has a lower electrophilicity than acetylacetone, and its activation is required to promote the condensation of another 1 equiv of a primary amine. Nonetheless, in the presence of a catalytic amount of sulfuric acid or PTSA, reaction of **2** and **1** (or 2,6-diisopropylaniline) led to a mixture of numerous products with loss of the conjugated keto-enamine backbone. In fact, **2a** is unstable in the presence of PTSA (1.0 mol %) and is transformed quantitatively to the benzoxazole derivative **3a** (Scheme 2, eq 2), within 24 h at 100 °C in toluene. **3a** has been successfully characterized by a combination of $^{1}H/^{13}C$ NMR spectroscopy and mass spectrometry (see the Experimental Section), and acetone is the only observed byproduct of this reaction ($^{1}H/^{13}C$ NMR). This transformation is unusual in the chemistry of keto-enamines and $\beta$-diketimines; yet, it is somewhat reminiscent of the rearrangement observed by Inamoto and co-workers for functionalized $\alpha$-diketimines, in the presence of oxidants.[13] A simple mechanistic model is proposed in Scheme 2. Protonation of the carbonyl group, by PTSA, is known to enhance the electrophilicity of the keto-enamine fragment in **2**.[1] While this activation is classically utilized to promote the condensation of an incoming primary amine, the intramolecular addition of the nucleophilic phenol group is favored in **2**. A series of equilibria, involving keto−enol tautomerism and prototropy, is then possible and leads to the formation of **3** after elimination of acetone. The driving force of the reaction is likely the formation of a stable aromatic benzoxazole heterocycle. In order to avoid formation of **3**, it is therefore necessary to avoid keto−enol tautomerism and/or prototropy equilibria preceding the irreversible elimination of acetone. Using a stoichiometric amount of triethyloxonium tetrafluoroborate,[14] alkylation of the carbonyl group in **2** cleanly resulted in the quantitative formation of the iminium salt **4**. Because the latter is highly sensitive toward moisture, the cation was not isolated but characterized, in solution, using $^{1}H/^{13}C$ NMR and reacted in situ with 1 molar equiv of **1** (or 2,6-diisopropylaniline). Although **4** is thermally stable and does not eliminate **3** and acetone, proton exchanges are made possible in the presence of a primary amine, and rearrangement to **3** was found to be competitive, with elimination of the iminium salt of the primary amine **5** as a byproduct (Scheme 3, eq 3), following a mechanism similar to the aforementioned rearrangement of **2a** to **3a** (see Scheme 3). As a result, utilization of **2** is unproductive in the formation of *N*-aryloxy-$\beta$-diketiminate ligands and ligands **II** are clearly unavailable using this synthetic scheme. Nonetheless, as presented in Scheme 3, unsymmetrical *N*-aryloxy-$\beta$-diketiminate ligands **I** can be prepared by introducing the *o*-aminophenol **1** in the second step of the condensation strategy, to avoid nucleophilic attack of the phenol group at the iminium functionality (see Scheme 4). In fact, reaction of the acnac pro-ligand **6**[7,11] with $Et_3OBF_4$ in $CH_2Cl_2$ at 25 °C yielded **7** within 1 h (Scheme 3, eq 4), which was isolated as a white solid and was fully characterized by $^{1}H/^{13}C$ NMR and X-ray diffraction analysis. Addition of **1a** or **1b** to a THF solution of **7** cleanly affords the protonated form of new functionalized $\beta$-diketiminate ligands **8** (Scheme 3, eq 4) in 85% yield for both **8a** and **8b**.

**Scheme 2. Synthesis of 2 and 3**

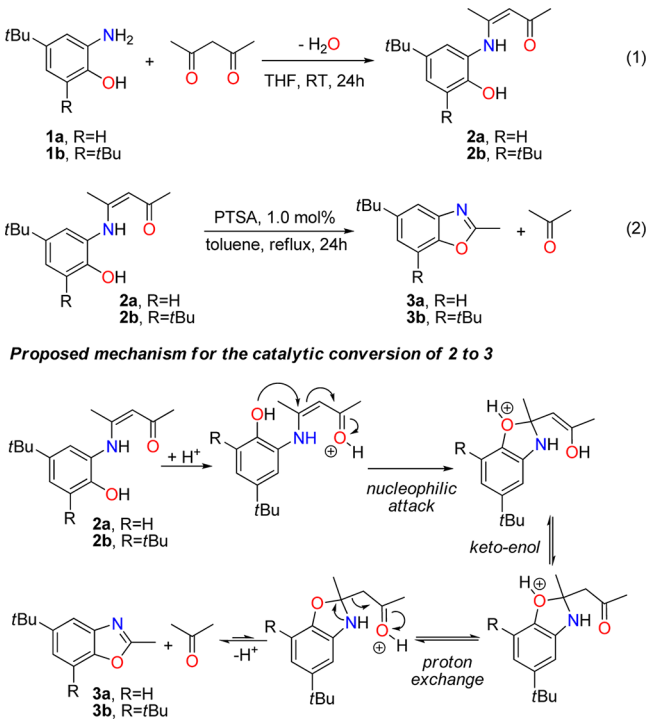


**Scheme 3. Successful and Unsuccessful Synthetic Approaches to 8a,b**[a]

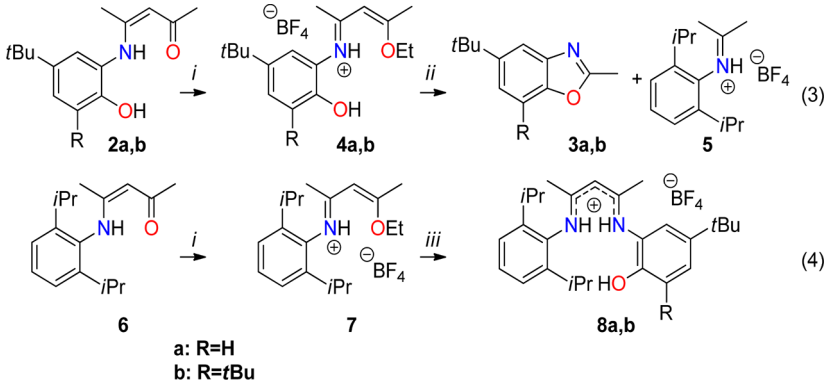


[a]Reaction conditions: (*i*) 1 equiv of $Et_3OBF_4$, $CH_2Cl_2$, room temperature, 1 h; (*ii*) (2,6-*i*$Pr_2$-$C_6H_4$)$NH_2$, $CH_2Cl_2$, room temperature, 1 h; (*iii*) **1a,b**, THF, room temperature, 1 h.


dx.doi.org/10.1021/om3010355 | *Organometallics* 2013, 32, 1328−1340

**Scheme 4. Proposed Mechanisms for the Selective Formation of 3a,b and 8a,b from 4a,b and 1a,b, Respectively**

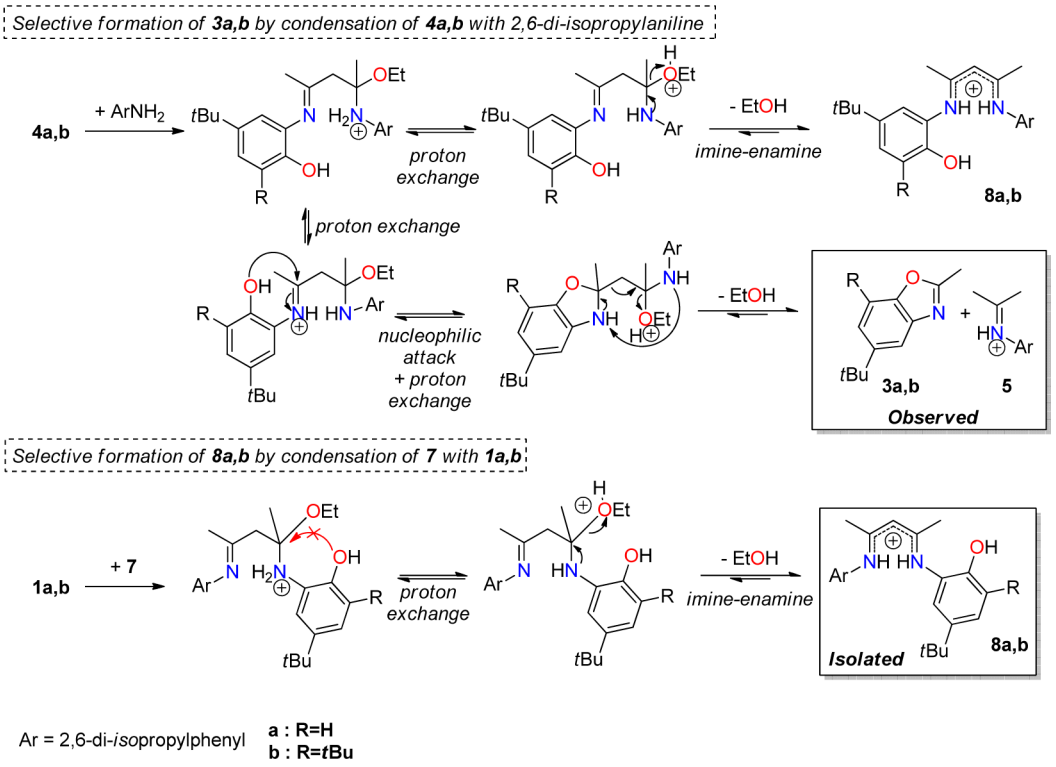


**Scheme 5. Synthesis of 9a**

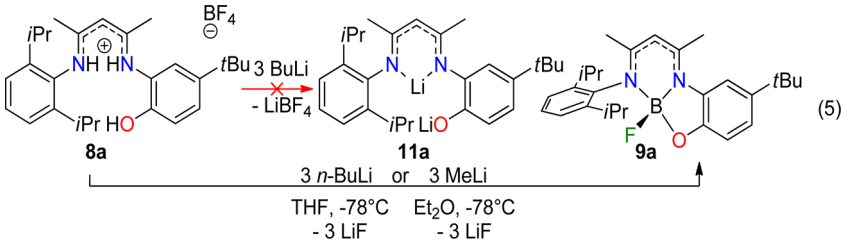


Deprotonation of **8a,b** was then attempted to prepare the dianionic *β*-diketiminate ligands. Unexpectedly, addition of 3 equiv of butyllithium to a THF solution of **8** at −78 °C results in the formation of the new borate species **9**, with elimination of LiF salt (Scheme 5, eq 5). Though the tetrafluoroborate anion is a stable counteranion, fluoride displacement at boron has been observed in rare instances and utilized for the synthesis of a handful of acac difluoroboron compounds.[15] While formation of **9b** was observed by $^{1}H/^{13}C$ NMR spectroscopy in a mixture of products (see the Experimental Section), **9a** was isolated by recrystallization from an acetonitrile solution and was fully characterized by X-ray diffraction (Figure 1), $^{1}H/^{13}C$ NMR spectroscopy, mass spectrometry, and elemental analysis. **9a** features a tetrahedral boron center substituted by one fluorine atom and one $\kappa^3$-coordinated *N*-aryloxy-*β*-diketiminate group. The B−F and B−N bond distances of 1.405(4) and 1.539(4) Å, respectively, fall in the range of isoelectronic boron−dipyrromethene (BODIPY) derivatives (average B−F and B−N distances of 1.39 and 1.55 Å, respectively).[16] Importantly, formation of **9a**, by deprotonation of **8a**, was also observed in the presence of chloride complexes, such as $ZrCl_4$ and $ThCl_4(DME)_2$. This suggests a greater stability of the boron derivative **9a** compared to the putative zirconium(IV) and thorium(IV) complexes. As

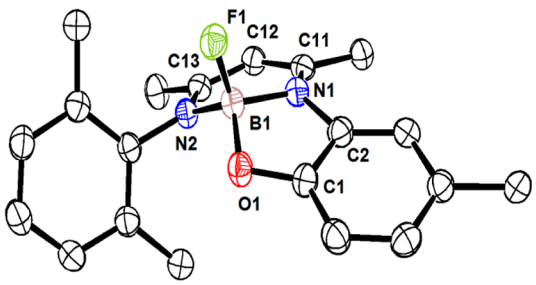


**Figure 1.** Molecular structure of **9a** with displacement ellipsoids drawn at the 50% probability level. Hydrogen atoms and $CH_3$ groups of the *i*Pr and *t*Bu substituents have been omitted. Selected bond distances (Å) and angles (deg): O1−B1 = 1.462(4), N1−B1 = 1.539(4), N2−B1 = 1.538(4), B1−F1 = 1.405(4), N1−C11 = 1.347(4), C11−C12 = 1.387(4), C12−C13 = 1.403(4), C13−N2 = 1.343(4); N1−C11−C12 = 118.3(3), C11−C12−C13 = 122.8(3), C12−C13−N2 = 120.7(3).

the presence of a $BF_4^-$ anion in **8** proved detrimental to the synthesis of the *N*-aryloxy-*β*-diketiminate dianions, successive deprotonation reactions were conducted so as to eliminate the counteranion prior to the formation of the anionic phenoxide and *β*-diketiminate donors (Scheme 6). Deprotonation of **8a** with 1 equiv of $NEt_3$, in $Et_2O$, led to the immediate formation


dx.doi.org/10.1021/om3010355 | *Organometallics* 2013, 32, 1328−1340

**Scheme 6. Synthesis of 10a,b and 11a,b**[a]

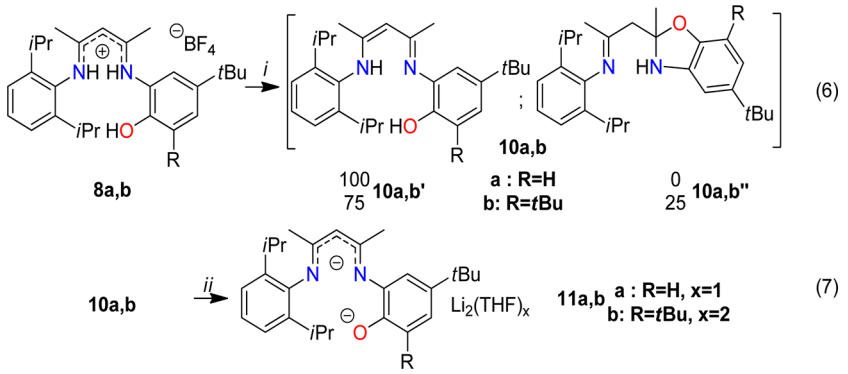


[a]Reaction conditions: (*i*) $NEt_3$, $Et_2O$, room temperature, 1 h; (*ii*) *n*-BuLi, THF, −78 °C.

of pro-ligand **10a** (Scheme 6, eq 6), with the concomitant precipitation of the $HNEt_3BF_4$ salt. After filtration and solvent evaporation, **10a** was isolated as a yellow oil and characterized by $^1H/^{13}C$ NMR spectroscopy and elemental analyses. **10b** was also isolated following the same transformation. However, **10b** was found to exist as a mixture of the two isomers **10b′** and **10b″** in a 3:1 ratio. While the *β*-diketimine form is predominant (**10b′**), a minor cyclic isomer (**10b″**) featuring a dihydrobenzoxazole group was found present both in solution and in the solid state and its structure was unambiguously established by X-ray diffraction analysis on monocrystals obtained by recrystallization of **10b** in cold (−40 °C) pentane (see the Experimental Section). Fortunately, cyclization of **10b′** to **10b″** was found to be reversible and addition of 2 molar equiv of *n*-butyllithium to **10b** yielded the unique dianion **11b** (Scheme 6, eq 7). Similarly, **11a** was quantitatively obtained from **10a**. Following this synthetic scheme, the desired *N*-aryloxy-*β*-diketiminate dianions **11a,b** were successfully prepared on multigram scales (>5.0 g), with an overall yield higher than 75% from commercially available compounds. The centrosymetric dimeric structure of **11a** is shown in Figure 2. It differs from that of **11b** by the number of coordinated lithium cations to the oxygen atom of the phenoxy group.[11] While the phenoxy donor O(1) in **11a** bridges three lithium ions, it is bound to two cations in the more congested *t*Bu derivative **11b**. Overall, the two monomeric units in **11a** are linked not only by the bridging phenolic oxygen atom O(1) between Li(1), Li(1′), and Li(2′) but also by the THF oxygen atom O(2) between Li(2) and Li(1′). The *β*-diketiminate fragment is planar in the usual U-shaped conformation, and this plane also contains the Li(2) atom, linked to N(1) and N(2) (rms deviation of 0.08 Å). Delocalization of the charge within the *β*-diketiminate backbone is indicated by the average C−C and C−N distances of 1.41(2) and 1.33(2) Å, respectively.

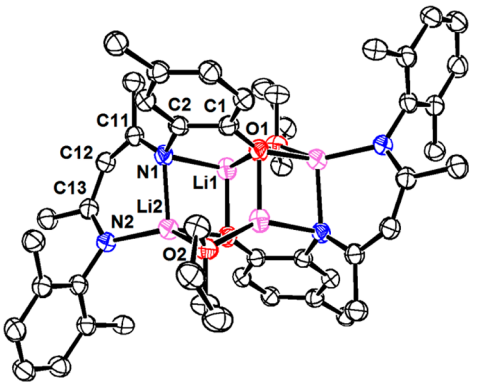


**Figure 2.** Molecular structure of **11a** with displacement ellipsoids drawn at the 50% probability level. Hydrogen atoms and $CH_3$ groups of the *i*Pr and *t*Bu substituents have been omitted. Symmetry code: (′) $1-x, 1-y, 2-z$. Selected bond distances (Å) and angles (deg): N1−C11 = 1.344(2), N2−C13 = 1.320(2), C11−C12 = 1.397(2), C12−C13 = 1.422(2), Li1−N1 = 2.111(3), Li1−O1 = 1.929(3), Li1−O1′ = 1.896(3), Li2−N1 = 2.018(3), Li2−N2 = 1.983(3), Li2−O2 = 2.275(3), Li2−O1′ = 1.905(3); N1−C11−C12 = 124.0(2), C11−C12−C13 = 129.2(2), C12−C13−N2 = 125.0(2).

**Coordination Chemistry.** Preliminary results gathered using dianion **11b** showed that the *N*-aryloxy-*β*-diketiminate ligand belongs to the $LX_2$ covalent bond classification and is able to support zirconium(IV), ytterbium(III), and thorium(IV) chloride complexes. Having in hand two versions of **11** with different steric bulks in the plane of the ligand (**11a**, R = H; **11b**, R = *t*Bu), we have investigated the differences in coordination chemistry between the two series and prepared the first uranium complexes of the *N*-aryloxy-*β*-diketiminate ligands. Salt metathesis reactions between **11a** and $ZrCl_4$, $YbCl_3$, and $ThCl_4(DME)_2$ (in a 1:1 ratio) afforded **12a−14a**, respectively (eqs 8−10 in Scheme 7). Under similar reaction conditions, complexes **12b−14b** were obtained using **11b** as a starting material and described in a preliminary communication.[11] The X-ray crystal structure of zirconium complex **12a**, depicted in Figure 3, is reminiscent of the structure obtained for **12b**, with a dimeric structure featuring two hexacoordinated zirconium(IV) centers supported by a $\kappa^3$-coordinated *N*-aryloxy-*β*-diketiminate ligand. However, while the metal coordination sphere is completed by one terminal and two bridging chloride ligands in **12b**, the phenoxy donor acts as the bridging ligand in **12a**. This different coordination behavior most likely results from a greater steric hindrance in the dianion of **11b**, which possesses a bulky *t*Bu group in the plane of the *N*-aryloxy-*β*-diketiminate backbone. This observation is also noticeable in the X-ray structures of the ytterbium(III) (**13a**, Figure 4) and thorium(IV) (**14a**, Figure 5) complexes. Interestingly, although the reaction of **11b** with $YbCl_3$ in pyridine affords a monomeric $Yb^{III}$ complex (**13b**), whose coordination sphere is saturated by three pyridine molecules, a dimeric complex (**13a**) is obtained when **11a** is used in place of **11b**, also in pyridine. The bond distances and angles in **12a−14a** are unexceptional and similar to the parameters found in the analogous complexes **12b−14b**. Noticeably, while the *N*-


dx.doi.org/10.1021/om3010355 | *Organometallics* 2013, 32, 1328−1340

**Scheme 7. Synthesis of 12a−14a and Structures of 12b−14b**[11]

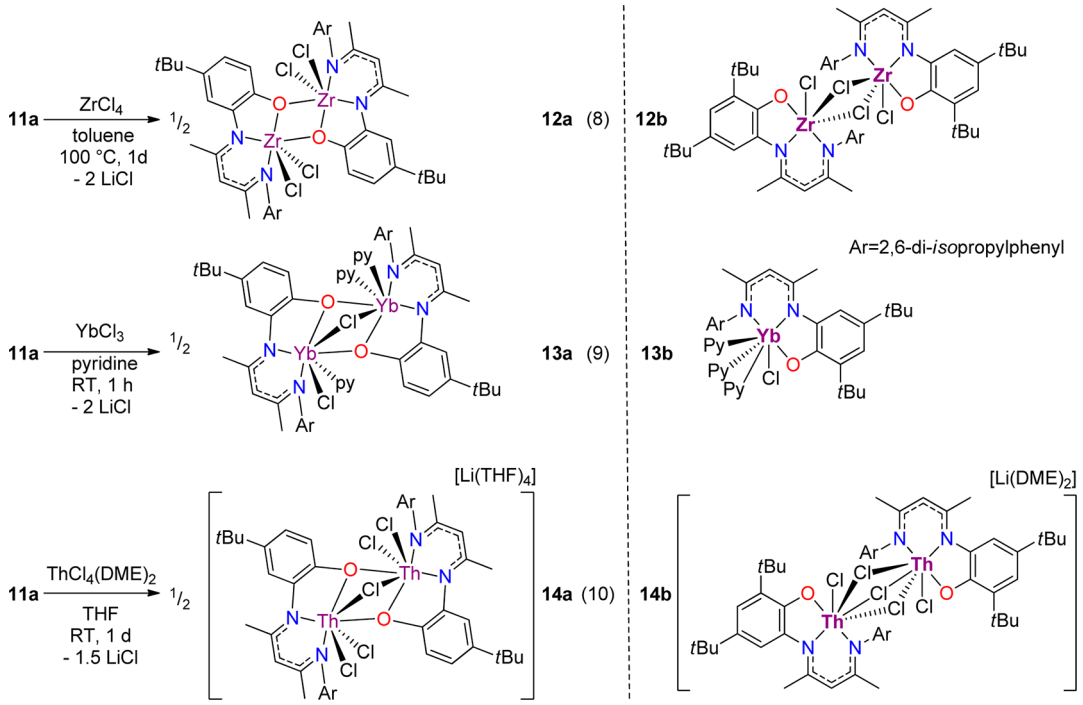


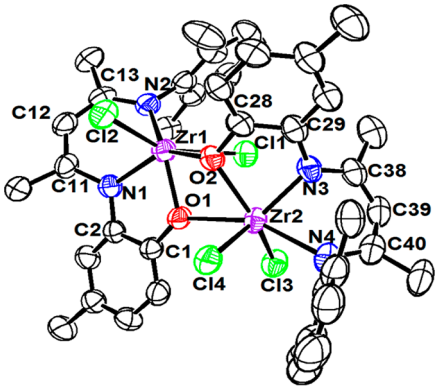


**Figure 3.** Molecular structure of **12a** with displacement ellipsoids drawn at the 50% probability level. Hydrogen atoms and $CH_3$ groups of the *i*Pr and *t*Bu substituents have been omitted. Selected bond distances (Å) and angles (deg): N1−C11 = 1.381(7), N2−C13 = 1.337(7), C11−C12 = 1.366(8), C12−C13 = 1.394(9), Zr1−N1 = 2.129(4), Zr2−N3 = 2.112(4), Zr1−N2 = 2.243(5), Zr2−N4 = 2.326(5), Zr1−O1 = 2.119(4), Zr2−O2 = 2.214(4); N1−C11−C12 = 121.6(2), C11−C12−C13 = 129.3(6), C12−C13−N2 = 121.7(5).

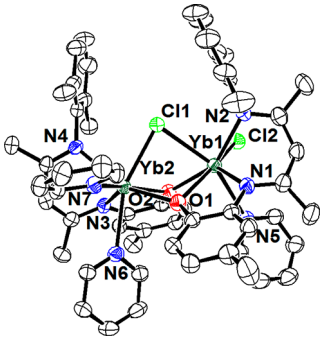


**Figure 4.** Molecular structure of **13a** with displacement ellipsoids drawn at the 50% probability level. Hydrogen atoms and $CH_3$ groups of the *i*Pr and *t*Bu substituents have been omitted. Selected bond distances (Å): Yb1−O1 = 2.325(3), Yb2−O2 = 2.260(3), Yb1−N1 = 2.275(4), Yb2−N3 = 2.240(4), Yb1−N2 = 2.398(4), Yb2−N4 = 2.418(4), Yb1−Cl1 = 2.6726(12), Yb2−Cl1 = 2.6329(12), N1−C11 = 1.346(6), C11−C12 = 1.405(7), C12−C13 = 1.439(7), C13−N2 = 1.318(6).

aryloxy-*β*-diketiminate behaves as a $LX_2$-type ligand in **12** and **13**, the *β*-diketiminate fragment is $\eta^5$ coordinated in **14a** and the ligand is $L_2X_2$, with an average Th−C distance of 3.0(1) Å.[11,17] These features are similar to those observed and discussed previously for the analogous **14b** compound.[11]

Despite the widespread use of *β*-diketiminate ligands in transition metal and lanthanide coordination chemistry,[1] *β*-diketiminate complexes of uranium are limited to a handful of examples, namely uranium(III,VI) and uranyl(V) complexes.[18−21] The *N*-aryloxy-*β*-diketiminate pincer anions **11** being successful precursors for the synthesis of thorium *β*-diketiminate complexes **14**, their coordination behavior toward $UI_4$(1,4-dioxane)$_2$ was investigated. While addition of **11a** to $UI_4$(1,4-dioxane)$_2$ led to the formation of a mixture of intractable products, a 1:1 mixture of the uranium(IV) iodide complex and **11b** afforded **15b** as the sole *N*-aryloxy-*β*-diketiminate complex. As revealed by the X-ray structure depicted in Figure 6, **15b** is a six-coordinate complex with a uranium(IV) cation stabilized by two $\kappa^3$-*N*-aryloxy-*β*-diketiminate ligands. It was therefore conveniently prepared, in 89% isolated yield, from a 2:1 mixture of **11b** and $UI_4$(1,4-dioxane)$_2$ (eq 11, Scheme 8). This reaction shows that, despite the steric congestion induced by the *t*Bu substituent on the phenoxide donor, bis complexes of the *N*-aryloxy-*β*-diketiminate ligand **11b** are available. Examples of complexes featuring two *N*-aryloxy-*β*-diketiminate ligands are not limited to **15b**, and using the same stoichiometry, the analogous zirconium(IV), ytterbium(III), and thorium(IV) complexes **16b−18b**, respectively, were synthesized (eqs 12−14 in Scheme 8). **16b** and **18b** are isostructural with **15b** (see structures in the Supporting


dx.doi.org/10.1021/om3010355 | *Organometallics* 2013, 32, 1328−1340

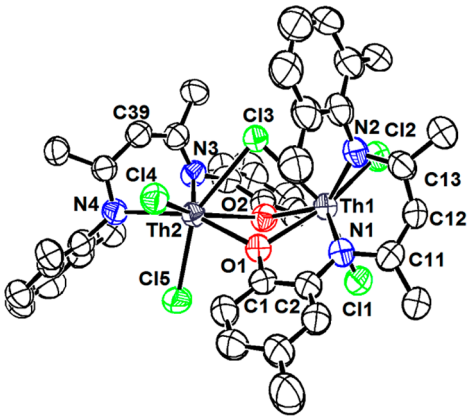


**Figure 5.** Molecular structure of **14a** with displacement ellipsoids drawn at the 50% probability level. Hydrogen atoms, $CH_3$ groups of the *i*Pr and *t*Bu substituents, and countercation $Li(THF)_4$ have been omitted. Selected bond distances (Å): Th1−O1 = 2.436(6), Th2−O2 = 2.475(6), Th1−N1 = 2.360(8), Th2−N3 = 2.407(8), Th1−N2 = 2.512(7), Th2−N4 = 2.508(7), Th1−Cl3 = 2.833(2), Th2−Cl3 = 2.914(2), Th1−C12 = 2.983(10), Th2−C39 = 2.977(9), N1−C11 = 1.35(2), C11−C12 = 1.39(2), C12−C13 = 1.44(8), C13−N2 = 1.34(2).

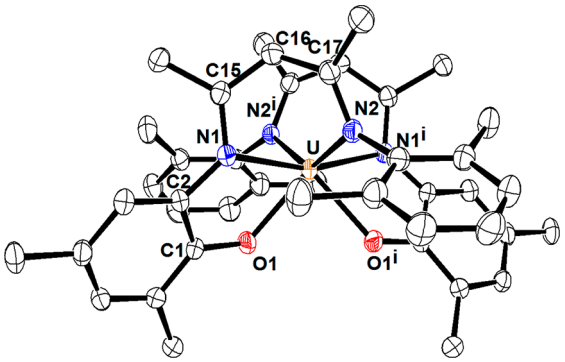


**Figure 6.** Molecular structure of **15b** with displacement ellipsoids drawn at the 50% probability level. Hydrogen atoms and $CH_3$ groups of the *i*Pr and *t*Bu substituents have been omitted. Symmetry code: (i) $1 - x, y, {}^3/_2 - z$. Selected bond distances (Å): U−O1 = 2.1900(13), U−N1 = 2.3679(17), U−N2 = 2.4566(16), U−C16 = 3.097, N1−C15 = 1.325(2), C15−C16 = 1.408(3), C16−C17 = 1.425(3), C17−N2 = 1.321(2).

Information), and the X-ray structure of **17b**, obtained by diffusion of pentane into a $Et_2O$ solution, is represented in Figure 7. In **15b**−**18b**, the *N*-aryloxy-*β*-diketiminate ligand is $\kappa^3$ coordinated and the metal−oxygen and metal−nitrogen bond distances are unexceptional and follow the trend expected from the change in metal ionic radius. In complexes **15b**, **16b**, and **18b**, the metal ion adopts a pseudo-trigonal-prismatic coordination geometry, as exemplified by trigonal twist angles $\theta$ (defined as the mean angle between the medians of the two trigonal faces defined by atoms O(1), N(1), and N($2^i$) and their image by the inversion center for the other face) close to 0° ($\theta$ < 13°; see Scheme 10). As a result, the metal ion is significantly displaced from the plane defined by the three donor atoms of the *N*-aryloxy-*β*-diketiminate ligand (1.42(1) Å in **15b**, 1.36(1) Å in **16b**, 1.44(1) Å in **18b**). In contrast, the anionic ytterbium(III) complex **17b** is best described as a pseudo-octahedron with a trigonal twist angle $\theta$ of 50.9° and the $Yb^{3+}$ ion is located in the plane of the pincer ligand

**Scheme 8. Synthesis of 15b−18b**

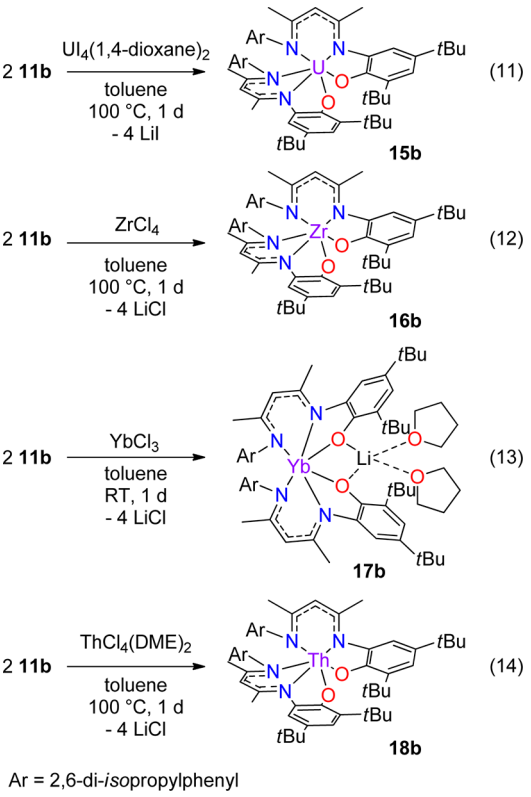


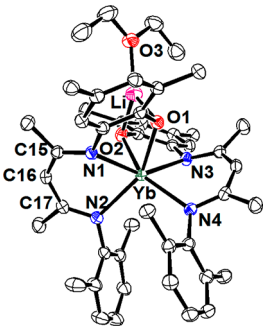


**Figure 7.** Molecular structure of **17b** crystallized from a $Et_2O$ solution (THF molecules from **17b** have been displaced by $Et_2O$ solvent upon crystallization). The displacement ellipsoids are drawn at the 50% probability level. Hydrogen atoms and $CH_3$ groups of the *i*Pr and *t*Bu substituents have been omitted. Selected bond distances (Å): Yb−O1 = 2.2242(12), Yb−O2 = 2.2345(12), Yb−N1 = 2.3507(13), Yb−N3 = 2.3425(14), Yb−N2 = 2.3792(14), Yb−N4 = 2.3725(14), N1−C15 = 1.329(2), C15−C16 = 1.412(2), C16−C17 = 1.403(2), C17−N2 = 1.346(2).

(deviation of 0.18(1) Å). Given that formation of coordination polyhedra is primarily governed by electrostatic interactions in the f-element series,[22] these structural differences likely result from the presence of a chelated lithium cation in the X-ray structure of **17b** and not from specific covalent interactions.

Synthesis of the bis(*N*-aryloxy-*β*-diketiminate) complexes with the less hindered **11a** dianion was subsequently attempted. Reaction of 2 equiv of **11a** with $ThCl_4(DME)_2$ in THF solution gave a mixture of numerous *N*-aryloxy-*β*-diketiminate complexes, among which the tris(*N*-aryloxy-*β*-diketiminate)-thorium(IV) complex **19a** crystallized, in small amounts, at 25 °C following slow diffusion of *n*-pentane over a $Et_2O$


dx.doi.org/10.1021/om3010355 | *Organometallics* 2013, 32, 1328−1340

solution of the crude mixture. The X-ray structure of **19a**, depicted in Figure 8, reveals the coordination of three *N*-

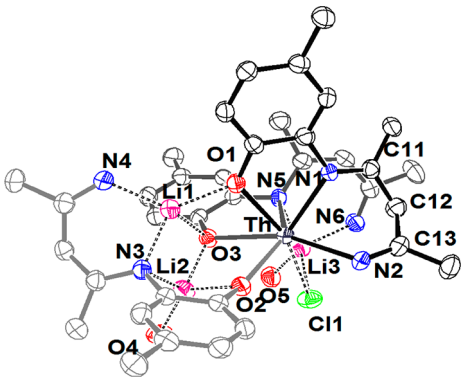


**Figure 8.** Molecular structure of **19a** with displacement ellipsoids drawn at the 50% probability level. Hydrogen atoms, $CH_3$ groups of the *t*Bu substituents, 2,6-diisopropylphenyl groups, and carbon atoms of diethyl ether (O5) and tetrahydrofuran (O4) have been omitted. The three $\beta$-diketiminate ligands are depicted in different shades of gray, and the bonds between lithium cations and N or O donors are dashed for easier description. Selected bond distances (Å) ($\kappa^3$-$\beta$-diketiminate ligand−Th, black): Th−O1 = 2.356(2), Th−N1 = 2.418(3), Th−N2 = 2.581(3), Th−C12 = 3.221, N1−C11 = 1.334(4), C11−C12 = 1.407(5), C12−C13 = 1.427(5), C13−N2 = 1.311(4).

aryloxy-$\beta$-diketiminate ligands and the presence of three lithium cations and one chloride anion. The $Th^{IV}$ ion is supported by three *N*-aryloxy-$\beta$-diketiminate ligands and one chloride ligand. While one *N*-aryloxy-$\beta$-diketiminate ligand is $\kappa^3$ coordinated, a second $\beta$-diketiminate ligand is $\kappa^2$(O,N) coordinated with the extra nitrogen donor coordinated to a lithium cation. Finally, the last *N*-aryloxy-$\beta$-diketiminate ligand interacts with the actinide atom via a bridging $\mu$-phenoxide donor. This aggregation state most probably results from the lower steric hindrance of the phenoxy group in **11a** compared to **11b**, and each of the three phenoxide donors in **19a** bridges one lithium and one thorium ion. Nonetheless, for the smaller zirconium(IV) (ionic radius (ir) = 0.72 Å vs 0.94 Å for $Th^{4+}$) and ytterbium(III) (ir = 0.87 Å), synthesis of bis(*N*-aryloxy-$\beta$-diketiminate) complexes is possible and **16a** and **17a** were isolated in 87 and 82% yields from $ZrCl_4$ and $YbCl_3$, respectively (eqs 15 and 16 in Scheme 9). Low carbon elemental analyses were observed for compounds **11a**, **13a**, **14a**, **16a**, and **17a** (with good H and N EAs) even on isolated monocrystals. We believe that LiCl is not a contaminant in

**Scheme 9. Synthesis of 16a and 17a**

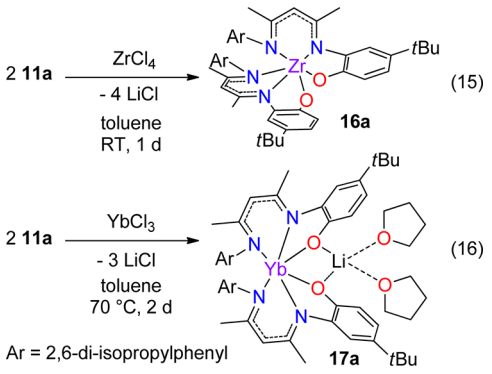


these samples, as the analogous **11b**−**17b** complexes, prepared following a similar synthetic route, yielded satisfactory EAs. In addition, good EAs were obtained for zirconium complex **12a**. Though X-ray-quality crystals could not be obtained for **17a**, the structure of **16a** was established by X-ray diffraction and is presented in Figure 9. Unlike **16b**, the coordination polyhedron

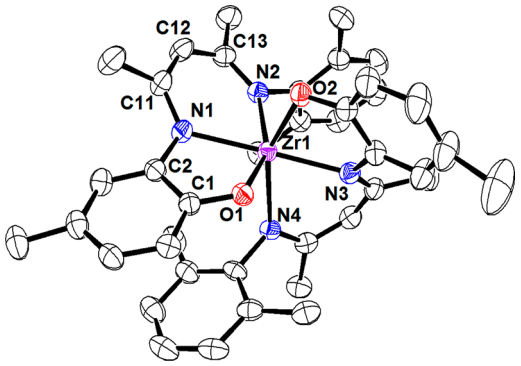


**Figure 9.** Molecular structure of **16a** with displacement ellipsoids drawn at the 50% probability level. Hydrogen atoms and $CH_3$ groups of the *i*Pr and *t*Bu substituents have been omitted. Selected bond distances (Å): Zr1−O1 = 2.011(2), Zr1−O2 = 2.029(2), Zr1−N1 = 2.289(3), Zr1−N3 = 2.225(3), Zr1−N2 = 2.259(3), Zr1−N4 = 2.258(3), N1−C11 = 1.337(5), C11−C12 = 1.400(6), C12−C13 = 1.395(5), C13−N2 = 1.337(5).

in **16a** is best described as a pseudo-octahedron with a trigonal twist of $\theta$ = 40.5° compared to 9.2° in **16b** (Scheme 10). Again, this difference in coordination behavior between the two *N*-aryloxy-$\beta$-diketiminate classes of ligands (R = H vs tBu) presumably has geometric origins. It is indeed well established that deviation from the stable octahedron to the trigonal prism is classically favored in the presence of chelate ligands with increased steric congestion and that the distortion minimizes the repulsion between ligands.[23−25]

**Scheme 10**

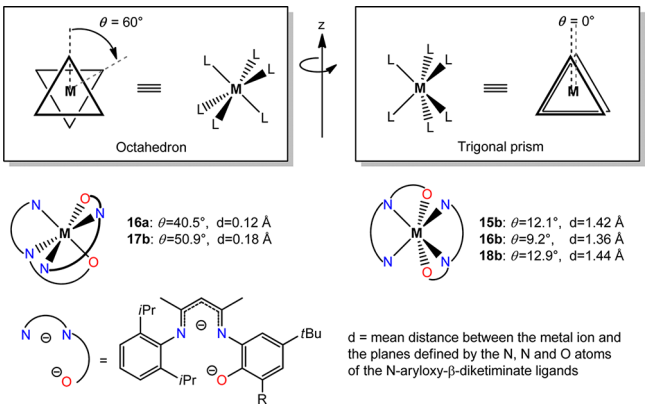


## CONCLUSION

Two examples of *N*-aryloxy-$\beta$-diketiminate ligands have been synthesized on a multigram scale, in four steps, from commercially available chemicals. The synthetic scheme relies on the sequential addition of 2,6-diisopropylaniline and 2-amino-4-*tert*-butylphenol (or 2-amino-4,6-di-*tert*-butylphenol) to acetylacetone, using $Et_3OBF_4$ as an activation reagent. Both the nature of the activation reagent and the order of addition of


dx.doi.org/10.1021/om3010355 | *Organometallics* 2013, 32, 1328−1340

the primary amines have a major impact on the outcome of the reaction, and acid catalysts (such as sulfuric acid or *p*-toluenesulfonic acid) lead to decomposition of the *β*-diketiminate backbone. Using dianions **11a**,**b**, mono- and bis(*N*-aryloxy-*β*-diketiminate) complexes of zirconium(IV), ytterbium(III), thorium(IV), and uranium(IV) have been synthesized, by salt metathesis reactions. The two ligands differ in their steric bulk and exhibit different coordination behaviors, which were rationalized on the basis of geometric considerations. We are presently exploring the potential of these new ligands in supporting catalysts and complexes featuring metal−main-group-element multiple bonds within the f-element series.

## EXPERIMENTAL SECTION

Unless otherwise noted, all reactions and manipulations were performed at 20 °C in a recirculating mBraun LabMaster DP inert-atmosphere (Ar) drybox and vacuum Schlenk lines. Glassware was dried overnight at 120 °C before use. All NMR spectra were obtained using a Bruker DPX 200 MHz spectrometer. Chemical shifts for $^{1}H$ and $^{13}C\{^{1}H\}$ NMR spectra were referenced to solvent impurities. Elemental analyses were performed at Analytische Laboratorien at Lindlar (Germany) and Medac Ltd. at Chobham (United Kingdom). Mass spectrometer data were collected on a Shimadzu GCMS-QP2010 Ultra gas chromatograph mass spectrometer equipped with a Supelco SLB-ms fused silica capillary column (30 m × 0.25 mm × 0.25 μm). Unless otherwise noted, reagents were purchased from commercial suppliers and dried over 4 Å molecular sieves prior to use. Celite (Aldrich) and 4 Å molecular sieves (Aldrich) were dried under dynamic vacuum at 250 °C for 48 h prior to use. Tetrahydrofuran (THF), tetrahydrofuran-$d_8$ (THF-$d_8$), *n*-pentane, diethyl ether, and benzene-$d_6$ were dried over a sodium(0)/benzophenone mixture and distilled before use. Pyridine and pyridine-$d_5$ were dried over potassium(0) prior to use. Triethylamine, dichloromethane, and dichloromethane-$d_2$ were dried over $CaH_2$ and distilled before use. $ThCl_4$(1,4-dimethoxyethane)$_2$,[26] $UI_4$(1,4-dioxane)$_2$,[27] **1b**,[11] **2b**,[11] **5**,[11] **6**,[7,11] **8b**,[11] **12b**,[11] **14b**,[11] and **15b**[11] were prepared according to literature procedures.

*Caution!* Natural thorium (primary isotope $^{232}Th$) is a weak *α* emitter (4.012 MeV) with a half-life of $1.41 \times 10^{10}$ years, and depleted uranium (primary isotope $^{238}U$) is a weak *α* emitter (4.197 MeV) with a half-life of $4.47 \times 10^{9}$ years; manipulations and reactions should be carried out in monitored fume hoods or in an inert-atmosphere drybox in a radiation laboratory equipped with *α*- and *β*-counting equipment.

**Synthesis of 2a.** A 100 mL round-bottom flask was charged with a stir bar, acetylacetone (1.7 mL, 17 mmol), 2-amino-4-*tert*-butylphenol **1a** (1.0 g, 6.1 mmol), and THF (10 mL). The resulting solution was sheltered from light and stirred for 24 h at room temperature. Solvent and excess acetylacetone were removed at 50 °C under reduced pressure to give a light yellow solid. Pentane (50 mL) was added, and the suspension was immersed in an ultrasound bath (80 W, 40 kHz) for 10 min, yielding a white solid and a brown solution. The solid was filtered off at −40 °C and washed with cold (−40 °C) pentane (10 mL) to afford **2a** as a white powder (0.96 g, 63%). Colorless translucent crystals were obtained by slow diffusion of pentane into a THF solution. $^{1}H$ NMR ($CD_2Cl_2$, 298 K): *δ* 1.26 (s, 9H, $C(CH_3)_3$); 1.82 (s, 3H, *α*-$CH_3$); 2.04 (s, 3H, *α*-$CH_3$); 5.19 (s, 1H, *β*-CH); 6.88 (d, *J* = 8.0 Hz, 1H, Ar-H); 7.04 (d, *J* = 2.0 Hz, 1H, Ar-H); 7.21 (dd, *J* = 2.0 Hz, 8.0 Hz, 1H, Ar-H); 8.16 (s, 1H, OH); 11.7 ppm (s, 1H, NH). $^{13}C$ NMR (THF-$d_8$, 298 K): *δ* 19.3 (s, *α*-$CH_3$); 28.7 (s, *α*-$CH_3$); 31.6 (s, $C(CH_3)_3$); 34.4 (s, $C(CH_3)_3$); 97.0 (s, *β*-CH); 116.4 (s, Ar); 124.4 (s, Ar); 124.7 (s, Ar); 126.6 (s, Ar); 142.8 (s, Ar); 150.6 (s, Ar); 161.7 (s, C−NH); 194.8 ppm (s, C−O).

**Synthesis of 3a.** A 125 mL round-bottom flask was charged with a stir bar, **2a** (150 mg, 0.606 mmol), *p*-toluenesulfonic acid hydrate (1.1 mg, 1% mol), and toluene (10 mL). The solution was stirred overnight at 90 °C. The volatiles were then removed under reduced pressure to yield the benzoxazole **3a** (115 mg, 100%). $^{1}H$ NMR ($C_6D_6$, 298 K): *δ* 1.21 (s, 9H, $C(CH_3)_3$); 2.10 (s, 3H, $CH_3$); 7.16 (m, 2H, Ar-H); 7.85 ppm (s, 1H, Ar-H). $^{13}C$ NMR ($C_6D_6$, 298 K): *δ* 14.0 (s, $CH_3$); 31.8 (s, $C(CH_3)_3$); 34.8(s, $C(CH_3)_3$); 109.5 (s, Ar); 116.8 (s, Ar); 122.2 (s, Ar); 147.5 (s, Ar); 149.7 (s, Ar); 163.9 ppm (s, C=N). GC/MS (EI; *m*/*z*): 189 ($M^+$, 21), 174 (100), 146 (24), 133 (26).

**Synthesis of 3b.** A 125 mL round-bottom flask was charged with a stir bar, **2b** (185 mg, 0.606 mmol), *p*-toluenesulfonic acid hydrate (1.1 mg, 1% mol), and toluene (10 mL). The solution was stirred at 90 °C for 2 days. The volatiles were then removed under reduced pressure to yield the benzoxazole **3b** (150 mg, 100%). $^{1}H$ NMR ($C_6D_6$, 298 K): *δ* 1.29 (s, 9H, $C(CH_3)_3$); 1.48 (s, 9H, $C(CH_3)_3$); 1.58 (acetone); 2.14 (s, 3H, $CH_3$); 7.37 (s, 1H, Ar-H); 7.78 ppm (s, 1H, Ar-H).

**Synthesis of 4a.** A 25 mL flask was charged with a stir bar, **2a** (500 mg, 2.02 mmol), triethyloxonium tetrafluoroborate (384 mg, 2.02 mmol), and methylene chloride (1 mL). The reaction mixture was stirred at room temperature for 1 h, generating in situ the *O*-alkylated cationic intermediate in a yellow solution. The volatiles were then removed under reduced pressure to yield the intermediate **4a**, directly used for further synthesis of **3a** and **5**. $^{1}H$ NMR ($CD_2Cl_2$, 298 K): *δ* 1.28 (s, 9H, $C(CH_3)_3$); 1.51 (t, *J* = 8.0 Hz, 3H, $OCH_2CH_3$); 2.38 (s, 6H, *α*-$CH_3$); 4.51 (q, *J* = 6.0 Hz, 2H, $OCH_2CH_3$); 5.63 (s, 1H, *β*-CH); 7.08−7.38 (m, 3H, Ar-H); 7.80 (br s, 1H, OH); 11.2 ppm (s, 1H, NH). $^{13}C$ NMR ($CD_2Cl_2$, 298 K): *δ* 14.8 (s, $OCH_2CH_3$); 20.7 (s, *α*-$CH_3$); 21.8 (s, *α*-$CH_3$); 31.3 (s, $C(CH_3)_3$); 34.4 (s, $C(CH_3)_3$); 69.5 (s, $OCH_2CH_3$); 101.0 (s, *β*-CH); 117.0 (s, Ar); 122.1 (s, Ar); 122.3 (s, Ar); 128.3 (s, Ar); 144.1 (s, Ar); 148.2 (s, Ar); 175.4 (s, C=N); 181.0 ppm (s, C=O).

**Synthesis of 4b.** A 100 mL flask was charged with a stir bar, **2b** (5.62 g, 21.7 mmol), triethyloxonium tetrafluoroborate (4.12 g, 21.7 mmol), and methylene chloride (13 mL). The reaction mixture was stirred at room temperature for 1 h, generating in situ the *O*-alkylated cationic intermediate in a brown-orange solution. The volatiles were then removed under reduced pressure to yield the intermediate **4b**, directly used for further synthesis of **3b** and **5**. $^{1}H$ NMR ($CD_2Cl_2$, 298 K): *δ* 1.29 (s, 9H, $C(CH_3)_3$); 1.38 (s, 9H, $C(CH_3)_3$); 1.46 (t, *J* = 8.0 Hz, 3H, $OCH_2CH_3$); 2.24 (s, 3H, *α*-$CH_3$); 2.38 (s, 3H, *α*-$CH_3$); 4.53 (q, *J* = 8.0 Hz, 2H, $OCH_2CH_3$); 5.68 (s, 1H, *β*-CH); 6.76 (br s, 1H, OH); 6.97 (d, *J* = 2.0 Hz, 1H, Ar-H); 7.42 (d, *J* = 2.0 Hz, 1H, Ar-H); 10.9 ppm (br s, 1H, NH). $^{13}C$ NMR ($CD_2Cl_2$, 298 K): *δ* 14.8 (s, $OCH_2CH_3$); 21.0 (s, *α*-$CH_3$); 21.7 (s, *α*-$CH_3$); 29.7 (s, $C(CH_3)_3$); 30.1 (s, $C(CH_3)_3$); 34.8 (s, $C(CH_3)_3$); 35.7 (s, $C(CH_3)_3$); 69.6 (s, $OCH_2CH_3$); 101.1 (s, *β*-CH); 120.7 (s, Ar); 124.4 (s, Ar); 126.0 (s, Ar); 140.1 (s, Ar); 144.2 (s, Ar); 147.4 (s, Ar); 177.9 (s, C=N); 182.6 ppm (s, C=O).

**Synthesis of 3a and 5.** 2,6-Diisopropylaniline (19.7 μL, 0,104 mmol) was added to a dichloromethane solution of intermediate **4a** (0.104 mmol), and the reaction mixture was stirred for 2 days at 60 °C. The volatiles were then removed under reduced pressure. Toluene (2 mL) was added to the mixture, leading to the formation of two phases. Iminium salt **5** was found as the major compound in the lower phase (dark brown oil), while **3a** is the major constituent of the upper light brown solution. Differences between $^{13}C$ NMR spectra led to complete recognition of all products. $^{13}C$ NMR ($CD_2Cl_2$, 298 K) (crude mixture): *δ* 14.6 (s, $CH_3$, **3a**); 15.4 (s, $Et_2O$); 18.4 (s, EtOH); 23.1 (s, $CH(CH_3)_2$, **5**); 24.1 (s, $CH_3$, **5**); 26.1 (s, $CH_3$, **5**); 29.1 (s, $CH(CH_3)_2$, **5**); 31.4 (s, $CH(CH_3)_2$, **5**); 31.9 (s, $C(CH_3)_3$, **3a**); 35.1(s, $C(CH_3)_3$, **3a**); 58.4 (s, EtOH); 66.0 (s, $Et_2O$); 109.7 (s, Ar, **3a**); 115.9 (s, Ar, **3a**); 122.6 (s, Ar, **3a**); 125.3 (s, Ar, **5**); 130.4 (s, Ar, **5**); 131.8 (s, Ar, **5**); 141.4 (s, Ar, **3a**); 143.6 (s, Ar, **5**); 148.1 (s, Ar, **3a**); 149.3 (s, Ar, **3a**); 164.7 (s, C=N, **3a**); 197.6 ppm (s, $C=N^+$, **5**).

**Synthesis of 7.** A 100 mL flask was charged with a stir bar, **6** (5.62 g, 21.7 mmol), triethyloxonium tetrafluoroborate (4.12 g, 21.7 mmol), and methylene chloride (13 mL). The reaction mixture was stirred at room temperature for 1 h, generating in situ the *O*-alkylated cationic intermediate **2**. The volatiles were then removed under reduced pressure to yield intermediate **7**, directly used for further synthesis. Colorless translucent monocrystals suitable for X-ray diffraction analysis were collected from a THF/pentane solution of **7**. $^{1}H$ NMR ($C_6D_6$, 298 K): *δ* 1.13−120 (m, 9H, $CH(CH_3)_2$, $OCH_2CH_3$); 1.30 (d, *J* = 6.0 Hz, 6H, $CH(CH_3)_2$); 1.94 (s, 3H, *α*-$CH_3$); 2.03 (s, 3H, *α*-$CH_3$); 2.97 (m, 2H, $CH(CH_3)_2$); 4.07 (q, *J*= 6.0 Hz, 2H, $OCH_2CH_3$);


dx.doi.org/10.1021/om3010355 | *Organometallics* 2013, 32, 1328−1340

6.30 (s, 1H, $\beta$-CH); 7.12−7.36 (m, 3H, Ar-H); 11.2 ppm (s, 1H, NH). $^{13}$C NMR ($C_6D_6$, 298 K): $\delta$ 14.8 (s, $OCH_2CH_3$); 20.6 (s, $\alpha$-$CH_3$); 20.9 (s, $\alpha$-$CH_3$); 22.7 (s, $CH(CH_3)_2$); 24.0 (s, $CH(CH_3)_2$); 29.0 ($CH(CH_3)_2$); 68.9 (s, $OCH_2CH_3$); 100.2 (s, $\beta$-CH); 124.7 (s, Ar); 130.5 (s, Ar); 130.9 (s, Ar); 144.7 (s, Ar); 178.8 (s, C═N); 182.7 ppm (s, C═O).

**Synthesis of 8a.** After removal of the volatiles, **7** was directly reacted with 2-amino-4-*tert*-butylphenol (**1a**; 3.76 g, 22.8 mmol) in THF (13 mL) at room temperature. The resulting yellow suspension was vigorously stirred for 30 min at room temperature, leading to a complete dissolution of **1a**. After drying under reduced pressure for 12 h, pentane (150 mL) was added to the yellow-brown foam and the mixture was immersed in an ultrasound bath (80 W, 40 kHz) for 90 min, yielding a well-defined white suspension. The white solid was recovered by filtration and washed with cold (−40 °C) diethyl ether (3 × 30 mL) to afford **8a** as a white powder (9.16 g, 85%). Colorless translucent crystals were obtained by slow diffusion of pentane into a THF solution of **8a**. Anal. Calcd for $C_{27}H_{39}BF_4N_2O$: C, 65.59; H, 7.95; N, 5.67; Found: C, 65.05: H, 7.98; N, 5.60. $^1$H NMR (THF-$d_8$, 298 K): $\delta$ 1.02 (d, $J$ = 6.0 Hz, 6H, $CH(CH_3)_2$); 1.09 (d, $J$ = 6.0 Hz, 6H, $CH(CH_3)_2$); 1.13 (s, 9H, $C(CH_3)_3$); 2.63 (s, 3H, $\alpha$-$CH_3$); 2.72 (s, 3H, $\alpha$-$CH_3$); 2.80 (m, 2H, $CH(CH_3)_2$); 4.67 (s, 1H, $\beta$-CH); 6.58 (d, $J$ = 8.0 Hz, 1H, Ar-H); 6.81 (s, 1H, Ar-H); 7.03−7.28 (m, 4H, Ar-H); 8.13 (s, 1H, OH); 9.44 ppm (s, 2H, NH). $^{13}$C NMR (THF-$d_8$, 298 K): $\delta$ 21.9 (s, $\alpha$-$CH_3$); 23.4 (s, $\alpha$-$CH_3$); 24.4 (s, $CH(CH_3)_2$); 28.9 (s, $CH(CH_3)_2$); 31.5 (s, $C(CH_3)_3$); 34.4 (s, $C(CH_3)_3$); 92.2 (s, $\beta$-CH); 117.0 (s, Ar); 117.1 (s, Ar); 123.2 (s, Ar); 124.4 (s, Ar); 127.2 (s, Ar); 129.8 (s, Ar); 132.3 (s, Ar); 143.2 (s, Ar); 146.1 (s, Ar); 150.5 (s, C−OH); 172.0 (s, C═NH); 172.4 ppm (s, C═NH).

**Synthesis of 9a.** A 50 mL flask was charged with a stir bar, **8a** (2.15 g, 4.35 mmol), and solid methyllithium (335 mg, 15.22 mmol). Diethyl ether (10 mL) was condensed in, yielding a yellow solution with a white precipitate. The suspension was stirred for 7 days. The volatiles were then removed under reduced pressure, and THF (30 mL) was condensed in. The solid was removed from the resulting suspension by centrifugation. The volatiles were then removed under reduced pressure to afford **9a** as an air- and water-stable yellow powder (1.20 g, 64%). Yellow needles of **9a** were obtained by slow evaporation of a $CH_3CN$ solution of **9a**. Anal. Calcd for $C_{27}H_{36}BFN_2O$: C, 74.65; H, 8.35; N, 6.45. Found: C, 74.49; H, 8.35; N, 6.37. $^1$H NMR (THF-$d_8$, 298 K): $\delta$ 1.07 (d, $J$ = 4.0 Hz, 3H, $CH(CH_3)_2$); 1.10 (d, $J$ = 4.0 Hz, 3H, $CH(CH_3)_2$); 1.42 (pseudo-t, $J$ = 6.0 Hz, 6H, $CH(CH_3)_2$); 1.50 (s, 9H, $C(CH_3)_3$); 2.06 (s, 3H, $\alpha$-$CH_3$); 2.32 (m, 1H, $CH(CH_3)_2$); 2.81 (s, 3H, $\alpha$-$CH_3$); 3.50 (m, 1H, $CH(CH_3)_2$); 5.78 (s, 1H, $\beta$-CH); 6.84 (d, $J$ = 8.0 Hz, 1H, Ar-H); 7.22 (dd, $J$ = 8.0 Hz, 2.0 Hz, 1H, Ar-H); 7.31 (pseudo-t, $J$ = 4.0 Hz, 1H, Ar-H); 7.45 (s, 1H, Ar-H); 7.48 (d, $J$ = 2.0 Hz, 1H, Ar-H); 7.64 ppm (d, $J$ = 2.0 Hz, 1H, Ar-H). $^{13}$C NMR ($C_6D_6$, 298 K): $\delta$ 20.6 (s, $\alpha$-$CH_3$); 21.2 (s, $\alpha$-$CH_3$); 23.8 (s, $CH(CH_3)_2$); 24.0 (s, $CH(CH_3)_2$); 24.6 (s, $CH(CH_3)_2$); 25.9 (s, $CH(CH_3)_2$); 26.0 (s, $CH(CH_3)_2$); 28.8 (s, $CH(CH_3)_2$); 31.9 (s, $C(CH_3)_3$); 34.5 (s, $C(CH_3)_3$); 99.9 (s, $\beta$-CH); 112.8 (s, Ar); 113.7 (s, Ar); 123.2 (s, Ar); 124.1 (s, Ar); 124.7 (s, Ar); 133.5 (s, Ar); 136.6 (s, Ar); 141.2 (s, Ar); 145.6 (s, Ar); 146.6 (s, Ar); 153.0 (s, C−O); 156.7 (s, C═N); 161.3 ppm (s, C═N). MS: (EI; $m/z$): 434 ($M^+$, 24), 419 (22); 230 (60), 202 (100).

**Synthesis of 9b.** A 50 mL flask was charged with a stir bar, **8b** (821 g, 1.49 mmol), and diethyl ether (15 mL). *n*-Butyllithium (2.80 mL, 4.47 mmol) was slowly added at −78 °C under an argon flow, using a syringe. The reaction mixture was warmed to room temperature and stirred for 7 days. After decantation, an aliquot of the solution was analyzed by $^1$H NMR spectroscopy and **9b** was identified as the major compound among other degradation products.$^1$H NMR ($C_6D_6$, 298 K): $\delta$ 0.86 (dd, $J$ = 6.0 Hz, 2.0 Hz, 3H, $CH(CH_3)_2$); 1.24 (d, $J$ = 8.0 Hz, 3H, $CH(CH_3)_2$); 1.28 (d, $J$ = 8.0 Hz, 3H, $CH(CH_3)_2$); 1.34 (s, 9H, $C(CH_3)_3$); 1.44 (s, 9H, $C(CH_3)_3$); 1.60 (d, $J$ = 8.0 Hz, 3H, $CH(CH_3)_2$); 1.65 (s, 3H, $\alpha$-$CH_3$); 2.01 (s, 3H, $\alpha$-$CH_3$); 2.88 (m, 1H, $CH(CH_3)_2$); 3.88 (m, 1H, $CH(CH_3)_2$); 5.20 (s, 1H, $\beta$-CH); 7.01 (dd, $J$ = 6.0 Hz, 2.0 Hz, 1H, Ar-H); 7.16 (m, 1H, Ar-H); 7.21 (d, $J$ = 2.0 Hz, 1H, Ar-H); 7.24 (d, $J$ = 2.0 Hz, 1H, Ar-H); 7.32 ppm (d, $J$ = 2.0 Hz, 1H, Ar-H).

**Synthesis of 10a.** A 100 mL flask was charged with a stir bar, **8a** (2.76 g, 5.58 mmol), and diethyl ether (40 mL). Triethylamine (0.93 mL, 6.70 mmol) was slowly added to the white suspension using a syringe, leading to the immediate formation of a yellow suspension. The mixture was stirred for 1 h. The white solid of triethylamonium tetrafluoroborate was then filtered off through a Celite padded coarse frit, and the yellow solution was introduced into a 100 mL two-neck round-bottom flask. The volatiles were removed under reduced pressure overnight, leading to **10a** as a yellow oil (2.20 g, 97%). Anal. Calcd for $C_{27}H_{38}N_2O$: C, 79.76; H, 9.42; N, 6.89. Found: C, 79.38; H, 9.47; N, 7.08. $^1$H NMR ($C_6D_6$, 298 K): $\delta$ 1.13 (d, $J$ = 6.0 Hz, 6H, $CH(CH_3)_2$); 1.19 (d, $J$ = 6.0 Hz, 6H, $CH(CH_3)_2$); 1.28 (s, 9H, $C(CH_3)_3$); 1.66 (s, 3H, $\alpha$-$CH_3$); 1.91 (s, 3H, $\alpha$-$CH_3$); 3.23 (m, 2H, $CH(CH_3)_2$); 4.97 (s, 1H, $\beta$-CH); 7.04−7.22 (m, 6H, Ar-H); 9.16 ppm (br s, 1H, NH); no OH signal had been identified. $^{13}$C NMR ($C_6D_6$, 298 K): $\delta$ 20.6 (s, $\alpha$-$CH_3$); 21.0 (s, $\alpha$-$CH_3$); 22.9 (s, $CH(CH_3)_2$); 24.5 (s, $CH(CH_3)_2$); 28.8 (s, $CH(CH_3)_2$); 31.8 (s, $C(CH_3)_3$); 34.2 (s, $C(CH_3)_3$); 96.7 ($\beta$-CH); 114.9 (s, Ar); 121.3 (s, Ar); 122.6 (s, Ar); 123.6 (s, Ar); 126.5 (s, Ar); 133.2 (s, Ar); 139.7 (s, Ar); 139.7 (s, Ar); 143.0 (s, Ar); 143.1 (s, Ar); 148.0 (s, Ar); 161.4 (s, C−N); 164.7 ppm (s, C−N).

**Synthesis of 10b.** A 100 mL flask was charged with a stir bar, **8b** (2.31 g, 4.19 mmol), and diethyl ether (40 mL). Triethylamine (0.64 mL, 4.61 mmol) was slowly added to the white suspension using a syringe, leading to the immediate formation of a yellow suspension. The mixture was stirred for 1 h. The white solid of triethylamonium tetrafluoroborate was then filtered off through a Celite padded coarse frit, and the yellow solution was introduced into a 100 mL two-neck round-bottom flask. The volatiles were removed under reduced pressure overnight, leading to two isomeric forms (**10b′**:**10b″** 75:25) of **10b** as a yellow oil (1.94 g, 100%). Yellow monocrystals of the minor isomer **10b″** suitable for X-ray diffraction analysis were recovered by recrystallization of **10b** in pentane. Anal. Calcd for $C_{31}H_{46}N_2O$: C, 80.47; H, 10.02; N, 6.05. Found: C, 80.18; N, 10.22; H, 5.96. $^1$H NMR of **10b′** (THF-$d_8$, 298 K): $\delta$ 1.13 (d, $J$ = 6.0 Hz, 6H, $CH(CH_3)_2$); 1.22 (d, $J$ = 6.0 Hz, 6H, $CH(CH_3)_2$); 1.27 (s, 9H, $C(CH_3)_3$); 1.40 (s, 9H, $C(CH_3)_3$); 1.71 (s, 3H, $\alpha$-$CH_3$); 1.87 (s, 3H, $\alpha$-$CH_3$); 3.11 (m, 2H, $CH(CH_3)_2$); 5.04 (s, 1H, $\beta$-CH); 6.78 (s, 1H, OH); 6.90−7.25 (m, 5H, Ar-H); 12.1 ppm (s, 1H, NH). Partial $^1$H NMR of **10b″** (THF-$d_8$, 298 K): $\delta$ 1.36 (s, 9H, $C(CH_3)_3$); 1.64 (s, 3H, $CH_3$); 1.76 (s, 3H, $CH_3$); 5.54 ppm (s, 1H, NH). $^{13}$C NMR of **10b′** (THF-$d_8$, 298 K): $\delta$ 20.4 (s, $\alpha$-$CH_3$); 21.0 (s, $\alpha$-$CH_3$); 23.1 (s, $CH(CH_3)_2$); 24.5 (s, $CH(CH_3)_2$); 28.9 (s, $CH(CH_3)_2$); 29.7 (s, $C(CH_3)_3$); 31.8 (s, $C(CH_3)_3$); 34.7 (s, $C(CH_3)_3$); 35.5 (s, $C(CH_3)_3$); 97.0 (s, $\beta$-CH); 120.8 (s, Ar); 123.2 (s, Ar); 123.5 (s, Ar); 125.5 (s, Ar); 131.9 (s, Ar); 135.7 (s, Ar); 141.5 (s, Ar); 141.6 (s, Ar); 142.5 (s, Ar); 148.3 (s, C−OH); 162.2 (s, C-NH); 163.5 ppm (s, C−NH). $^{13}$C NMR of **10b″** (THF-$d_8$, 298 K): $\delta$ 22.8 (s, $CH(CH_3)_2$); 23.0 (s, $CH_3$); 23.4 (s, $CH(CH_3)_2$); 23.5 (s, $CH(CH_3)_2$); 23.8 (s, $CH(CH_3)_2$); 28.4 (s, $CH(CH_3)_2$); 28.6 (s, $CH(CH_3)_2$); 28.9 (s, $CH_3$); 29.8 (s, $C(CH_3)_3$); 32.1 (s, $C(CH_3)_3$); 34.5 (s, $C(CH_3)_3$); 35.0 (s, $C(CH_3)_3$); 48.9 (s, $CH_2C$═N); 101.1 (s, Ar); 108.4 (s, Ar); 115.1 (s, Ar); 123.6 (s, Ar); 124.1 (s, Ar); 131.0 (s, Ar); 136.6 (s, Ar); 136.7 (s, Ar); 139.1 (s, Ar); 142.5 (s, Ar); 146.5 (s, Ar); 146.7 (s, Ar); 170.1 ppm (s, C═N).

**Synthesis of 11a.** A 100 mL two-neck round-bottom flask was charged with a stir bar, **10a** (2.20 g, 5.41 mmol), and THF (20 mL). *n*-Butyllithium (6.80 mL, 10.8 mmol) was slowly added at −78 °C under an argon flow, using a syringe. The resulting deep yellow solution was warmed to room temperature, yielding an orange solution with a yellow precipitate. After concentration of the solution to 10 mL, the solid was filtered off and washed with cold pentane (2 × 10 mL, −40 °C), to provide **11a** as a yellow powder (2.82 g, 93%). Yellow crystals of **11a** were recovered by slow diffusion of pentane over a THF solution and used for further NMR analysis after moderate drying under reduced pressure to avoid desolvation. Anal. Calcd for $C_{27}H_{36}Li_2N_2O$·THF: C, 75.90; H, 9.04; N, 5.71. Found: C, 73.76; H, 9.54, N, 5.75. Several attempts of elemental analysis led to poor C correlation each time. $^1$H NMR ($C_6D_6$, 298 K): $\delta$ 1.22 (m, 12H, THF); 1.30 (pseudo-t, $J$ = 6.0 Hz, 12H, $CH(CH_3)_2$); 1.40 (s, 9H,


dx.doi.org/10.1021/om3010355 | *Organometallics* 2013, 32, 1328−1340

$C(CH_3)_3$); 1.91 (s, 3H, $\alpha$-$CH_3$); 2.18 (s, 3H, $\alpha$-$CH_3$); 3.34 (m, 12H, THF); (m, 2H, $CH(CH_3)_2$); 5.01 (s, 1H, $\beta$-CH); 6.70−7.20 ppm (m, 6H, Ar-H). $^{13}$C NMR ($C_6D_6$, 298 K): $\delta$ 24.1 (s, $\alpha$-$CH_3$); 24.4 (s, $\alpha$-$CH_3$); 25.5 (s, $CH(CH_3)_2$, THF); 28.2 (s, $CH(CH_3)_2$); 32.2 (s, $C(CH_3)_3$); 34.0 (s, $C(CH_3)_3$); 68.2 (s, THF); 96.8 (s, $\beta$-CH); 118.8 (s, Ar); 119.1 (s, Ar); 122.0 (s, Ar); 123.2 (s, Ar); 123.4 (s, Ar); 138.1 (s, Ar); 140.9 (s, Ar); 144.8 (s, Ar); 149.7 (s, Ar); 157.9 (s, Ar); 165.2 (s, C−N); 165.3 ppm (s, C−N).

**Synthesis of 11b.** A 100 mL two-neck round-bottom flask was charged with a stir bar, **10b** (2.50 g, 5.41 mmol), and THF (20 mL). *n*-Butyllithium (6.80 mL, 10.8 mmol) was slowly added at −78 °C under an argon flow, using a syringe. The resulting deep yellow solution was warmed to room temperature, yielding an orange solution with a yellow precipitate. After concentration of the solution to 10 mL, the solid was filtered off and washed with cold pentane (2 × 10 mL, −40 °C). **11b** was finally isolated as a pale yellow powder (3.18 g, 95%). Yellow crystals of [**11b**]$_2$·0.5(*n*-pentane) were obtained by slow diffusion of pentane into a THF solution. Elemental analyses were made with samples used in NMR spectroscopy with $C_6D_6$. Anal. Calcd for $C_{39}H_{60}Li_2N_2O_3$·0.5$C_6H_6$: C, 76.68; H, 9.65; N, 4.26. Found: C, 76.68; H, 9.62; N, 4.70. $^1$H NMR ($C_6D_6$, 298 K): $\delta$ 1.18 (d, $J$ = 8.0 Hz, 6H, $CH(CH_3)_2$); 1.26 (d, $J$ = 8.0 Hz, 6H, $CH(CH_3)_2$); 1.34 (s, 9H, $C(CH_3)_3$); 1.73 (s, 9H, $C(CH_3)_3$); 1.96 (s, 3H, $\alpha$-$CH_3$); 2.19 (s, 3H, $\alpha$-$CH_3$); 3.50 (m, 2H, $CH(CH_3)_2$); 5.14 (s, 1H, $\beta$-CH); 6.85 (d, $J$ = 2.0 Hz, 1H, Ar-H); 7.10−7.30 ppm (m, 4H, Ar-H). $^{13}$C NMR ($C_6D_6$, 298 K): $\delta$ 23.7 (s, $\alpha$-$CH_3$); 23.9 (s, $CH(CH_3)_2$); 24.2 (s, $CH(CH_3)_2$); 24.6 (s, $\alpha$-$CH_3$); 25.5 (s, THF); 28.2 (s, $CH(CH_3)_2$); 31.1 (s, $C(CH_3)_3$); 32.3 (s, $C(CH_3)_3$); 34.2 (s, $C(CH_3)_3$); 35.3 (s, $C(CH_3)_3$); 68.1 (s, THF); 98.0 (s, $\beta$-CH); 118.1 (s, Ar); 120.2 (s, Ar); 123.5 (s, Ar); 128.4 (s, Ar); 135.8 (s, Ar); 136.2 (s, Ar); 140.6 (s, Ar); 145.6 (s, Ar); 149.2 (s, Ar); 154.2 (s, C−O); 161.3(s, C═N); 170.2 ppm (s, C═N).

**Synthesis of 12a.** A 25 mL flask was charged with a stir bar, $ZrCl_4$ (159 mg, 0.682 mmol), **11a** (328 mg, 0.669 mmol), and toluene (15 mL). The orange suspension was heated to 100 °C for 1 day and then cooled to room temperature. The white precipitate of LiCl was filtered off over a fine-porosity fritted filter. The resulting red solution was dried under reduced pressure to provide a red-orange powder (315 mg, 83%). Red monocrystals were obtained by recrystallization from deuterated benzene, leading to [**12a**]$_2$·6.5$C_6D_6$ as a dimer. Anal. Calcd for $C_{27}H_{36}Cl_2N_2OZr$·$C_6D_6$: C, 61.47; H, 6.57; N, 4.34. Found: C, 60.98; H, 6.78; N, 4.55. $^1$H NMR ($C_6D_6$, 298 K): $\delta$ 0.89 (m, 12H, $CH(CH_3)_2$); 1.24 (s, 9H, $C(CH_3)_3$); 1.65 (s, 3H, $\alpha$-$CH_3$); 2.01 (s, 3H, $\alpha$-$CH_3$); 2.25 (m, 1H, $CH(CH_3)_2$); 3.82 (m, 1H, $CH(CH_3)_2$); 5.72 (s, 1H, $\beta$-CH); 6.69 (s, 1H, Ar-H); 7.04 (m, 4H, Ar-H), 8.08 ppm (d, $J$ = 6.0 Hz, 1H, Ar-H). $^{13}$C NMR ($C_6D_6$, 298 K): $\delta$ 21.5 (s, $\alpha$-$CH_3$); 22.1 (s, $\alpha$-$CH_3$); 24.1−24.3 (multiple broad signals, $CH(CH_3)_2$); 25.1 (s, $CH(CH_3)_2$); 31.7 (s, $C(CH_3)_3$); 34.4 (s, $C(CH_3)_3$); 111.9 (s, $\beta$-CH); 115.6 (s, Ar); 119.4 (s, Ar); 120.2 (s, Ar); 124.3 (s, Ar); 127.1 (s, Ar); 138.8 (s, Ar); 141.5 (s, Ar); 144.4 (s, Ar); 149.2 (s, Ar); 153.5 (s, Ar); 155.4 (s, C═N); 171.2 ppm (s, C═N).

**Synthesis of 13a.** A 25 mL flask was charged with a stir bar, $YbCl_3$ (229 mg, 0.819 mmol), **11a** (402 mg, 0.820 mmol), and pyridine (20 mL). The deep red solution was stirred for 1 h at room temperature and then concentrated to less than 1 mL. Toluene (20 mL) was condensed in and the white precipitate filtered off over a fine-porosity fritted filter. The resulting red solution was dried under reduced pressure to provide **13a** as a red-orange powder (580 mg, 97%). Red monocrystals of **13a** were recovered by slow diffusion of pentane over a pyridine solution of **13a**. Anal. Calcd for $C_{69}H_{87}Cl_2N_7O_2Yb_2$·0.5Py: C, 54.59; H, 5.95; N, 5.37. Found: C, 51.05; H, 5.98; N, 5.28. Several attempts at elemental analysis led to poor C correlation, including from isolated crystals. $^1$H NMR (pyridine-$d_5$, 298 K): $\delta$ −49.6 (br s, 1H); −33.1 (br s, 1H); −24.0 (br s, 3H); −21.5 (br s, 3H); −17.6 (br s, 6H); −15.2 (br s, 2H); −11.4 (br s, 6H); −2.3 (s, 9H); 18.7 (br s, 1H); 22.0 (br s, 1H); 23.0 (br s, 1H); 25.3 ppm (br s, 1H).

**Synthesis of 14a.** A 25 mL flask was charged with a stir bar, $ThCl_4(DME)_2$ (159 mg, 0.287 mmol), **11a** (141 mg, 0.287 mmol), and THF (15 mL). The yellow suspension was stirred for 12 h at room temperature and then concentrated to 1 mL. Toluene (25 mL) was added to the flask, the white precipitate of LiCl was filtered off over a fine-porosity fritted filter, and the yellow-orange solution was dried under reduced pressure to provide **14a** as a yellow powder (204 mg, 87%). Yellow monocrystals of **14a**·2THF were recovered by slow diffusion of pentane over a THF solution. **14a** is probably unstable over time in the solid state, which causes poor elemental analysis correlation. Anal. Calcd for $C_{62}H_{92}Cl_5LiN_4O_6Th_2$: C, 45.47; H, 5.66; N, 3.42. Found: C, 39.36; H, 5.43; N, 2.99. $^1$H NMR (pyridine-$d_5$, 298 K): $\delta$ 1.00−1.40 (m, 12H, $CH(CH_3)_2$); 1.36 (s, 9H, $C(CH_3)_3$); 2.20 (s, 3H, $\alpha$-$CH_3$); 2.58 (s, 3H, $\alpha$-$CH_3$); 5.70 (s, 1H, $\beta$-CH); 6.96 (s, 2H, Ar-H); 7.08 (m, 1H, Ar-H); 7.23 ppm (m, 3H, Ar-H); THF signals are missing due to the drying process. $^{13}$C NMR (THF-$d_8$, 298 K): $\delta$ 21.8 (s, $\alpha$-$CH_3$); 24.8 (s, $\alpha$-$CH_3$); (s, $CH(CH_3)_2$); 28.5 (br s, $CH(CH_3)_2$); 32.3 (s, $C(CH_3)_3$); 34.5 (s, $C(CH_3)_3$); 92.1 (s, $\beta$-CH); 114.8 (s, Ar); 117.5 (s, Ar); 119.9 (s, Ar); 123.3 (br s, Ar); 125.4 (s, Ar); 139.7 (s, Ar); 140.3 (s, Ar); 142.7 (br s, Ar); 148.4 (s, Ar); 154.3 (s, Ar); 160.4 (s, C═N); 165.6 ppm (s, C═N).

**Synthesis of 15b.** A 25 mL flask was charged with $UI_4$(1,4-dioxane)$_2$ (179 mg, 0.194 mmol), **11b** (240 mg, 0.388 mmol), and toluene (50 mL). The red suspension was heated to 100 °C for 12 h. The complex is poorly soluble in toluene and was extracted in a Soxhlet apparatus under an inert atmosphere using toluene and dried under reduced pressure to provide **15b** as a red powder (201 mg, 89%), which was recrystallized from toluene to afford dark red monocrystals. Anal. Calcd for $C_{62}H_{88}N_4O_2U$: C, 64.23; H, 7.65; N, 4.83. Found: C, 63.83; H, 7.70; N, 4.99. $^1$H NMR ($C_6D_6$, 298 K): $\delta$ −24.4 (s, 1H); −20.0 (s, 3H); −15.7 (s, 3H); −8.1 (s, 9H); −6.9 (s, 1H); −4.6 (s, 1H); −1.9 (s, 3H); −1.1 (s, 3H); 3.6 (s, 1H); 3.7 (s, 1H); 10.3 (s, 9H); 17.8 (s, 1H); 18.6 (s, 3H); 23.6 (s, 3H); 29.2 (s, 1H); 45.1 ppm (s, 1H).

**Synthesis of 16a.** A 25 mL flask was charged with a stir bar, $ZrCl_4$ (64.9 mg, 0.278 mmol), **11a** (273 mg, 0.557 mmol), and toluene (10 mL). The deep red suspension was stirred for 12 h at room temperature. The white precipitate was then filtered off over a fine-porosity fritted filter, and the volatiles were removed under reduced pressure to provide **16a** as a red powder (220 mg, 87%). Red monocrystals of [**16a**]$_2$·1.5(*n*-pentane) were recovered by recrystallization in pentane. Anal. Calcd for $C_{54}H_{72}N_4O_2Zr$: C, 72.03; H, 8.06; N, 6.22. Found: C, 70.12; H, 8.23; N, 6.16. As for ligand **11a**, poor C correlations were obtained while several attempts had been made, including with isolated monocrystals. $^1$H NMR ($C_6D_6$, 298 K): $\delta$ 1.03−1.25 (m, 12H, $CH(CH_3)_2$); 1.25(s, 9H, $C(CH_3)_3$); 1.60 (s, 3H, $\alpha$-$CH_3$); 1.89 (s, 3H, $\alpha$-$CH_3$); 3.25 (m, 2H, $CH(CH_3)_2$); 4.95 (s, 1H, $\beta$-CH); 6.31 (d, $J$ = 8.0 Hz, 1H, Ar-H); 6.68 (d, $J$ = 8.0 Hz, 1H, Ar-H); 6.75 (s, 1H, Ar-H); 7.01 ppm (m, 3H, Ar-H). $^{13}$C NMR ($C_6D_6$, 298 K): $\delta$ 23.7 (s, $\alpha$-$CH_3$); 24.4 (s, $\alpha$-$CH_3$); 25.5 (s, $CH(CH_3)_2$); 25.5 (s, $CH(CH_3)_2$); 25.7 (s, $CH(CH_3)_2$); 25.9 (s, $CH(CH_3)_2$); 28.0 (s, $CH(CH_3)_2$); 30.2 (s, $CH(CH_3)_2$); 31.9 (s, $C(CH_3)_3$); 34.1 (s, $C(CH_3)_3$); 105.6 (s, $\beta$-CH); 113.9 (s, Ar); 118.3 (s, Ar); 121.7 (s, Ar); 123.1 (s, Ar); 125.4 (s, Ar); 126.7 (s, Ar); 139.8 (s, Ar); 140.3 (s, Ar); 143.4 (s, Ar); 145.0 (s, Ar); 145.1 (s, Ar); 158.5 (s, Ar); 162.5 (s, C═N); 166.1 ppm (s, C═N).

**Synthesis of 16b.** A 25 mL flask was charged with a stir bar, $ZrCl_4$ (35.0 mg, 0.154 mmol), **11b** (191 mg, 0.308 mmol), and toluene (15 mL). The orange suspension was heated to 100 °C for 1 day and then cooled to room temperature. The white precipitate was filtered off over a fine-porosity fritted filter. The volatiles were then removed under reduced pressure to provide **16b** as an orange powder (145 mg, 93%). Orange monocrystals were obtained by recrystallization from toluene. Anal. Calcd for $C_{62}H_{88}N_4O_2Zr$: C, 73.54; H, 8.76; N, 5.53. Found: C, 73.42; H, 8.70; N, 5.53. $^1$H NMR (THF-$d_8$, 298 K): $\delta$ 0.81 (m, 21H, $CH(CH_3)_2$, $C(CH_3)_3$); 1.24 (s, 9H, $C(CH_3)_3$); 1.66 (s, 3H, $\alpha$-$CH_3$); 2.17 (br s, 3H, $\alpha$-$CH_3$); 3.01 (m, 2H, $CH(CH_3)_2$); 5.16 (s, 1H, $\beta$-CH); 6.71 (s, 2H, Ar-H); 7.00 ppm (m, 4H, Ar-H). $^{13}$C NMR ($C_6D_6$, 298 K): $\delta$ 23.0−26.5 (multiple broad signals, $\alpha$-$CH_3$, $CH(CH_3)_2$); 28.1 (s, $CH(CH_3)_2$); 30.2 (s, $C(CH_3)_3$); 32.1 (s, $C(CH_3)_3$); 34.5 (s, $C(CH_3)_3$); 34.9 (s, $C(CH_3)_3$); 118.6 (s, Ar); 123.7 (s, Ar); 125.2 (s, Ar); 126.5 (s, Ar); 131.2 (br s, Ar); 134.6 (s, Ar); 139.5 (s, Ar); 140−144 (multiple broad signals, Ar); 157.9 (s, C═N); 167.0 ppm (s, C═N).


dx.doi.org/10.1021/om3010355 | *Organometallics* 2013, 32, 1328−1340

**Table 1. Crystal Data and Structure Refinement Details**

| | 7 | 8a | 9a | 10b″ | 11a |
|---|---|---|---|---|---|
| chem formula | $C_{19}H_{30}BF_4NO$ | $C_{27}H_{39}BF_4N_2O$ | $C_{27}H_{36}BFN_2O$ | $C_{37}H_{52}N_2O$ | $C_{62}H_{88}Li_4N_4O_4$ |
| mol wt | 375.25 | 494.41 | 434.39 | 540.81 | 981.12 |
| cryst syst | orthorhombic | monoclinic | monoclinic | triclinic | triclinic |
| space group | $P2_12_12_1$ | $P2_1/n$ | $P2_1/n$ | $P\bar{1}$ | $P\bar{1}$ |
| $a$ (Å) | 10.5912(5) | 16.1246(13) | 18.9985(15) | 9.9061(6) | 9.5402(14) |
| $b$ (Å) | 14.0519(7) | 10.6141(11) | 6.8889(3) | 13.0594(10) | 10.9327(11) |
| $c$ (Å) | 14.0695(5) | 34.007(3) | 21.2758(16) | 14.8115(12) | 14.383(2) |
| $\alpha$ (deg) | 90 | 90 | 90 | 103.480(3) | 73.960(8) |
| $\beta$ (deg) | 90 | 100.304(6) | 115.889(3) | 108.736(4) | 87.426(7) |
| $\gamma$ (deg) | 90 | 90 | 90 | 103.910(4) | 86.955(9) |
| $V$ (Å$^3$) | 2093.91(16) | 5726.4(9) | 2505.1(3) | 1658.0(2) | 1439.0(3) |
| $Z$ | 4 | 8 | 4 | 2 | 1 |
| $D_{calcd}$ (g cm$^{-3}$) | 1.190 | 1.147 | 1.152 | 1.083 | 1.132 |
| $\mu$(Mo K$\alpha$) (mm$^{-1}$) | 0.096 | 0.086 | 0.074 | 0.064 | 0.068 |
| $F$(000) | 800 | 2112 | 936 | 592 | 532 |
| no. of rflns collcd | 35900 | 129840 | 78144 | 89409 | 40602 |
| no. of indep rflns | 2253 | 10853 | 4747 | 8571 | 5395 |
| no. of obsd rflns ($I > 2\sigma(I)$) | 2014 | 4873 | 3918 | 4688 | 3931 |
| $R_{int}$ | 0.026 | 0.070 | 0.027 | 0.049 | 0.051 |
| no. of params refined | 243 | 649 | 298 | 373 | 343 |
| R1 | 0.053 | 0.061 | 0.071 | 0.055 | 0.051 |
| wR2 | 0.154 | 0.147 | 0.174 | 0.145 | 0.137 |
| $S$ | 1.135 | 0.988 | 1.151 | 0.976 | 1.030 |
| $\Delta\rho_{min}$ (e Å$^{-3}$) | −0.21 | −0.19 | −0.24 | −0.21 | −0.19 |
| $\Delta\rho_{max}$ (e Å$^{-3}$) | 0.29 | 0.17 | 0.23 | 0.18 | 0.27 |

| | 12a | 13a | 14a | 15b | 16a | 19a |
|---|---|---|---|---|---|---|
| chem formula | $C_{90}H_{108}Cl_4N_4O_2Zr_2$ | $C_{74}H_{92}Cl_2N_8O_2Yb_2$ | $C_{74}H_{112}Cl_5LiN_4O_7Th_2$ | $C_{62}H_{88}N_4O_2U$ | $C_{59}H_{84}N_4O_2Zr$ | $C_{89}H_{126}ClLi_3N_6O_5Th$ |
| mol wt | 1602.04 | 1542.54 | 1817.95 | 1159.39 | 972.52 | 1648.27 |
| cryst syst | triclinic | monoclinic | triclinic | monoclinic | triclinic | triclinic |
| space group | $P\bar{1}$ | $P2_1/c$ | $P\bar{1}$ | $C2/c$ | $P\bar{1}$ | $P\bar{1}$ |
| $a$ (Å) | 17.4358(9) | 14.8213(7) | 15.8182(5) | 21.2552(10) | 15.5297(7) | 13.1462(6) |
| $b$ (Å) | 17.4360(12) | 21.6499(5) | 19.2508(5) | 10.7158(5) | 18.9498(9) | 16.4882(6) |
| $c$ (Å) | 32.131(2) | 24.1822(11) | 19.7418(6) | 25.9523(7) | 21.2327(9) | 23.2295(11) |
| $\alpha$ (deg) | 89.401(3) | 90 | 111.6569(12) | 90 | 75.631(2) | 97.148(2) |
| $\beta$ (deg) | 80.627(3) | 98.984(2) | 107.7145(14) | 102.364(3) | 78.574(3) | 104.141(2) |
| $\gamma$ (deg) | 65.259(4) | 90 | 101.935(2) | 90 | 70.549(2) | 113.277(2) |
| $V$ (Å$^3$) | 8734.9(10) | 7664.4(5) | 4964.6(3) | 5774.0(4) | 5661.8(5) | 4345.0(3) |
| $Z$ | 4 | 4 | 2 | 4 | 4 | 2 |
| $D_{calcd}$ (g cm$^{-3}$) | 1.218 | 1.337 | 1.216 | 1.334 | 1.141 | 1.260 |
| $\mu$(Mo K$\alpha$) (mm$^{-1}$) | 0.407 | 2.541 | 3.167 | 2.855 | 0.236 | 1.798 |
| $F$(000) | 3360 | 3128 | 1816 | 2384 | 2088 | 1716 |
| no. of rflns collcd | 292190 | 270809 | 179951 | 156817 | 200992 | 159943 |
| no. of indep rflns | 33105 | 19782 | 18483 | 8792 | 21468 | 16265 |
| no. of obsd rflns ($I > 2\sigma(I)$) | 20664 | 12225 | 13984 | 7705 | 15185 | 13674 |
| $R_{int}$ | 0.079 | 0.061 | 0.050 | 0.030 | 0.042 | 0.057 |
| no. of params refined | 1853 | 865 | 926 | 324 | 1299 | 975 |
| R1 | 0.073 | 0.044 | 0.079 | 0.025 | 0.054 | 0.036 |
| wR2 | 0.225 | 0.119 | 0.230 | 0.059 | 0.165 | 0.081 |
| $S$ | 1.033 | 1.010 | 1.044 | 0.989 | 1.064 | 1.022 |
| $\Delta\rho_{min}$ (e Å$^{-3}$) | −0.50 | −0.95 | −2.08 | −0.94 | −0.83 | −0.85 |
| $\Delta\rho_{max}$ (e Å$^{-3}$) | 1.33 | 1.27 | 6.02 | 0.90 | 1.88 | 1.03 |

| | 16b | 17b | 18b | 19a |
|---|---|---|---|---|
| chem formula | $C_{62}H_{88}N_4O_2Zr$ | $C_{70}H_{108}LiN_4O_4Yb$ | $C_{62}H_{88}N_4O_2Th$ | $C_{89}H_{126}ClLi_3N_6O_5Th$ |
| mol wt | 1012.58 | 1249.58 | 1153.40 | 1648.27 |
| cryst syst | monoclinic | monoclinic | monoclinic | triclinic |
| space group | $C2/c$ | $P2_1/c$ | $C2/c$ | $P\bar{1}$ |
| $a$ (Å) | 21.0006(3) | 16.0461(2) | 21.2874(9) | 13.1462(6) |
| $b$ (Å) | 10.7340(2) | 21.2603(5) | 10.7327(3) | 16.4882(6) |
| $c$ (Å) | 25.6378(5) | 20.5180(5) | 26.0590(11) | 23.2295(11) |
| $\alpha$ (deg) | 90 | 90 | 90 | 97.148(2) |


dx.doi.org/10.1021/om3010355 | Organometallics 2013, 32, 1328−1340

Table 1. continued

| | 16b | 17b | 18b | 19a |
|---|---|---|---|---|
| $\beta$ (deg) | 102.3059(6) | 107.9728(13) | 102.213(2) | 104.141(2) |
| $\gamma$ (deg) | 90 | 90 | 90 | 113.277(2) |
| $V$ (Å$^3$) | 5646.50(17) | 6658.1(2) | 5819.0(4) | 4345.0(3) |
| $Z$ | 4 | 4 | 4 | 2 |
| $D_{calcd}$ (g cm$^{-3}$) | 1.191 | 1.247 | 1.317 | 1.260 |
| $\mu$(Mo K$\alpha$) (mm$^{-1}$) | 0.240 | 1.453 | 2.606 | 1.798 |
| $F$(000) | 2176 | 2644 | 2376 | 1716 |
| no. of rflns collcd | 97610 | 229111 | 92726 | 159943 |
| no. of indep rflns | 5305 | 20303 | 7405 | 16265 |
| no. of obsd rflns ($I > 2\sigma(I)$) | 4787 | 16366 | 6173 | 13674 |
| $R_{int}$ | 0.021 | 0.032 | 0.044 | 0.057 |
| no. of params refined | 324 | 749 | 324 | 975 |
| R1 | 0.031 | 0.028 | 0.031 | 0.036 |
| wR2 | 0.081 | 0.069 | 0.063 | 0.081 |
| $S$ | 1.022 | 1.008 | 0.970 | 1.022 |
| $\Delta\rho_{min}$ (e Å$^{-3}$) | −0.44 | −1.19 | −1.40 | −0.85 |
| $\Delta\rho_{max}$ (e Å$^{-3}$) | 0.38 | 0.48 | 0.55 | 1.03 |

**Synthesis of 17a.** A 25 mL flask was charged with a stir bar, $YbCl_3$ (41.6 mg, 0.149 mmol), **11a** (146 mg, 0.298 mmol), and toluene (15 mL). The orange suspension was stirred at 70 °C for 2 days. The white precipitate of LiCl was then filtered off through a Celite padded coarse frit, and the volatiles were removed under reduced pressure to provide **17a** as a deep orange powder (108 mg, 82%). Anal. Calcd for $C_{62}H_{88}LiN_4O_4Yb$: C, 65.70; H, 7.83; N, 4.94. Found: C, 64.14; H, 7.98; N, 5.21. As for ligand **11a**, poor C correlations were obtained while several attempts had been made. $^1$H NMR (THF-$d_8$, 298 K): $\delta$ −40.9 (s, 1H); −36.1 (s, 3H); −17.1 (s, 1H); −6.8 (s, 9H); −5.0 (s, 3H); 4.6 (s, 1H); 8.8 (s, 3H); 13.6 (s, 1H); 13.7 (s, 1H); 15.1 (s, 3H); 15.4 (s, 3H); 18.4 (s, 3H); 21.1 (s, 1H); 21.6 (s, 1H); 45.0 (br s, 1H); 78.1 ppm (br s, 1H).

**Synthesis of 17b.** A 25 mL flask was charged with a stir bar, $YbCl_3$ (26.4 mg, 0.0945 mmol), **11b** (117 mg, 0.189 mmol), and toluene (15 mL). The yellow-orange suspension was stirred for 12 h at room temperature. The white precipitate was then filtered off through a Celite padded coarse frit, and the volatiles were removed under reduced pressure to provide **17b** as a deep orange powder (108 mg, 82%). Orange monocrystals of **17b**·$Et_2O$, with Li($Et_2O$) countercation instead of Li(THF)$_2$, were recovered by slow diffusion of pentane over a diethyl ether solution of **17b** and were analyzed using NMR spectroscopy. Anal. Calcd for $C_{70}H_{104}LiN_4O_4Yb$: C, 67.50; H, 8.42; N, 4.50. Found: C, 67.83; H, 8.32; N, 4.65. $^1$H NMR ($C_6D_6$, 298 K): $\delta$ −45.1 (s, 1H); −27.1 (s, 3H); −22.9 (s, 1H); −14.5 (s, 3H); −8.0 (s, 3H); −5.6 (m, 1H+2H($Et_2O$)); −2.56 (s, 3H); 2.1 (s, 2H); 3.7 (s, 9H, C($CH_3$)$_3$); 7.1 (m, 3H, $Et_2O$); 7.7 (s, 1H); 14.2 (s, 3H); 15.0 (s, 9H, C($CH_3$)$_3$); 17.5 (s, 1H); 20.5 (s, 1H); 37.2 ppm (s, 3H).

**Synthesis of 18b.** A 25 mL flask was charged with a stir bar, $ThCl_4(DME)_2$ (239 mg, 0.431 mmol), **11b** (534 mg, 0.862 mmol), and toluene (25 mL). The orange suspension was heated to 100 °C for 1 day and then cooled to room temperature. The white precipitate was filtered off over a fine-porosity fritted filter. The volatiles were removed under reduced pressure to provide **18b** as a yellow powder (495 mg, 99%). Yellow monocrystals were recovered by recrystallization from toluene. Anal. Calcd for $C_{62}H_{88}N_4O_2Th$: C, 64.56; H, 7.69; N, 4.86. Found: C, 64.34; H, 7.65; N, 4.92. $^1$H NMR ($C_6D_6$, 298 K): $\delta$ 1.03 (dd, $J$ = 4.0 Hz, 6.0 Hz, 6H, CH(C$H_3$)$_2$); 1.24 (s, 9H, C($CH_3$)$_3$); 1.25 (dd, $J$ = 4.0 Hz, 6.0 Hz, 6H, CH(C$H_3$)$_2$); 1.34 (s, 9H, C($CH_3$)$_3$); 1.66 (s, 3H, $\alpha$-$CH_3$); 2.02 (s, 3H, $\alpha$-$CH_3$); 3.02 (m, 2H, C$H$($CH_3$)$_2$); 4.69 (s, 1H, $\beta$-CH); 6.77 (d, $J$ = 2.0 Hz, 1H, Ar-H); 7.03 (m, 3H, Ar-H); 7.12 ppm (s, 1H, Ar-H). $^{13}$C NMR ($C_6D_6$, 298 K): $\delta$ 23.4 (s, $\alpha$-$CH_3$); 24.6 (s, CH(C$H_3$)$_2$); 24.9 (s, CH(C$H_3$)$_2$); 25.1 (s, CH(C$H_3$)$_2$); 25.7 (s, $\alpha$-$CH_3$); 25.8 (s, CH(C$H_3$)$_2$); 28.8 (s, CH(C$H_3$)$_2$); 30.2 (s, C($CH_3$)$_3$); 31.5 (s, CH(C$H_3$)$_2$); 32.1 (s, C($CH_3$)$_3$); 34.4 (s, C($CH_3$)$_3$); 35.0 (s, C($CH_3$)$_3$); 97.5 (s, $\beta$-CH); 117.4 (s, Ar); 119.1 (s, Ar); 124.3 (s, Ar); 124.9 (s, Ar); 126.3 (s, Ar); 128.4 (s, Ar); 135.8 (s, Ar); 139.0 (s, Ar); 140.5 (s, Ar); 142.6 (s, Ar); 143.3 (s, Ar); 157.0 (s, C−O); 160.2 (s, C═N); 165.1 ppm (s, C═N).

**Structure Determination by X-ray Diffraction.** The data were collected at 150(2) K on a Nonius Kappa-CCD area detector diffractometer[28] using graphite-monochromated Mo K$\alpha$ radiation ($\lambda$ = 0.71073 Å). The crystals were introduced into glass capillaries with a protecting "Paratone-N" oil (Hampton Research) coating. The unit cell parameters were determined from 10 frames and then refined on all data. The data (combinations of $\varphi$ and $\omega$ scans with a minimum redundancy of 4 for 90% of the reflections) were processed with HKL2000.[29] Absorption effects were corrected empirically with the program SCALEPACK,[29] except for the compounds containing only light atoms. The structures were solved by direct methods or Patterson map interpretation with SHELXS-97 (except when an isostructural model could be used as a starting point), expanded by subsequent Fourier-difference synthesis, and refined by full-matrix least squares on $F^2$ with SHELXL-97.[30] All non-hydrogen atoms were refined with anisotropic displacement parameters. When present, the hydrogen atoms bound to oxygen or nitrogen atoms were found on Fourier difference maps. The carbon-bound hydrogen atoms were introduced at calculated positions; all hydrogen atoms were treated as riding atoms with an isotropic displacement parameter equal to 1.2 times that of the parent atom (1.5 for $CH_3$). In the absence of a suitable anomalous scatterer in **7**, the Friedel pairs have been merged. In both **12a** and **14a**, one *tert*-butyl substituent was found to be rotationally disordered over two positions, which were refined with occupancy parameters constrained to sum to unity. In **12a**−**14a**, some solvent molecules were given an occupancy parameter of 0.5 in order to retain acceptable displacement parameters. Voids in the lattice of **14a** likely indicate the presence of other, unresolved solvent molecules. Crystal data and structure refinement parameters are given in Table 1. The molecular plots were drawn with ORTEP-3.[31]

## ■ ASSOCIATED CONTENT

### Ⓢ Supporting Information

CIF files giving atomic positions and displacement parameters, anisotropic displacement parameters, and bond lengths and bond angles. This material is available free of charge via the Internet at http://pubs.acs.org.

## ■ AUTHOR INFORMATION

### Corresponding Author

*E-mail: thibault.cantat@cea.fr. Fax: +33 1 6908 6640. Tel: +33 1 6908 4338.

### Notes

The authors declare no competing financial interest.

## ■ ACKNOWLEDGMENTS

For financial support of this work, we acknowledge the CEA, CNRS, ANR (Starting Grant to T.C.) and GNR PARIS (Research Grant to T.C.).

## ■ REFERENCES

(1) Bourget-Merle, L.; Lappert, M. F.; Severn, J. R. *Chem. Rev.* **2002**, *102*, 3031−3066.
(2) Gunanathan, C.; Milstein, D. *Acc. Chem. Res.* **2011**, *44*, 588−602.
(3) Peris, E.; Crabtree, R. H. *Coord. Chem. Rev.* **2004**, *248*, 2239−2246.
(4) Poyatos, M.; Mata, J. A.; Peris, E. *Chem. Rev.* **2009**, *109*, 3677−3707.
(5) Lappert, M. F.; Liu, D.-S. Neth. Patent 9401515, 1994.
(6) Lappert, M. F.; Liu, D.-S. Neth. Patent 9500085, 1995.
(7) Dove, A. P.; Gibson, V. C.; Marshall, E. L.; White, A. J. P.; Williams, D. J. *Dalton Trans.* **2004**, 570−578.
(8) Neculai, A. M.; Neculai, D.; Roesky, H. W.; Magull, J. *Polyhedron* **2004**, *23*, 183−187.
(9) Bertrand, J. A.; Helm, F. T.; Carpenter, L. J. *Inorg. Chim. Acta* **1974**, *9*, 69−75.
(10) Lu, E.; Gan, W.; Chen, Y. *Organometallics* **2009**, *28*, 2318−2324.
(11) Dulong, F.; Bathily, O.; Thuéry, P.; Ephritikhine, M.; Cantat, T. *Dalton Trans.* **2012**, *41*, 11980−11983.
(12) Feldman, J.; McLain, S. J.; Parthasarathy, A.; Marshall, W. J.; Calabrese, J. C.; Arthur, S. D. *Organometallics* **1997**, *16*, 1514−1516.
(13) Yoshifuji, M.; Nagase, R.; Inamoto, N. *Bull. Chem. Soc. Jpn.* **1982**, *55*, 873−876.
(14) Piesik, D. F.-J.; Range, S.; Harder, S. *Organometallics* **2008**, *27*, 6178−6187.
(15) Mayoral, M. J.; Cano, M.; Campo, J. A.; Heras, J. V.; Pinilla, E.; Torres, M. R. *Inorg. Chem. Commun.* **2004**, *7*, 974−978.
(16) Sakida, T.; Yamaguchi, S.; Shinokubo, H. *Angew. Chem., Int. Ed.* **2011**, *50*, 2280−2283.
(17) Hitchcock, P. B.; Hu, J.; Lappert, M. F.; Tian, S. *J. Organomet. Chem.* **1997**, *536*−*537*, 473−480.
(18) Schettini, M. F.; Wu, G.; Hayton, T. W. *Inorg. Chem.* **2009**, *48*, 11799−11808.
(19) Wright, R. J.; Power, P. P.; Scott, B. L.; Kiplinger, J. L. *Organometallics* **2004**, *23*, 4801−4803.
(20) Hayton, T. W.; Wu, G. *J. Am. Chem. Soc.* **2008**, *130*, 2005−2014.
(21) Hitchcock, P. B.; Lappert, M. F.; Liu, D.-S. *J. Organomet. Chem.* **1995**, *488*, 241−248.
(22) Burns, C. J.; Bursten, B. E. *Comments Inorg. Chem.* **1989**, *9*, 61−93.
(23) Lesnard, H.; Cantat, T.; Le Floch, P.; Demachy, I.; Jean, Y. *Chem. Eur. J.* **2007**, *13*, 2953−2965.
(24) Cremades, E.; Echeverría, J.; Alvarez, S. *Chem. Eur. J.* **2010**, *16*, 10380−10396.
(25) Alvarez, S.; Avnir, D.; Llunell, M.; Pinsky, M. *New J. Chem.* **2002**, *26*, 996−1009.
(26) Cantat, T.; Scott, B. L.; Kiplinger, J. L. *Chem. Commun.* **2010**, *46*, 919−921.
(27) Monreal, M. J.; Thomson, R. K.; Cantat, T.; Travia, N. E.; Scott, B. L.; Kiplinger, J. L. *Organometallics* **2011**, *30*, 2031−2038.
(28) Hooft, R. Nonius BV, Delft, The Netherlands, 1998.
(29) Otwinowski, Z.; Minor, W. In *Methods in Enzymology*; Charles, W., Carter, J., Eds.; Academic Press: New York, 1997; Vol. *276*, pp 307−326.
(30) Sheldrick, G. M. *Acta Crystallogr., Sect. A: Found. Crystallogr.* **2007**, *64*, 112−122.
(31) Farrugia, L. J. *J. Appl. Crystallogr.* **1997**, *30*, 565−565.